Vascular Changes in the Supraspinatus Muscle and Association with Intramuscular Fat Accumulation: An Experimental Study in Rabbits

By Meaghan MacIntyre-Newell

Thesis submitted to the University of Ottawa in partial fulfillment of the requirements for the degree of Master of Science, Biology

Supervisor
Dr. Odette Laneuville

Department of Biology
Faculty of Science
University of Ottawa

© Meaghan MacIntyre-Newell, Ottawa, Canada, 2018

ABSTRACT

Supraspinatus (SSP) tendon tear leads to intramuscular fat accumulation in the SSP muscle and the mechanisms are currently unknown. The purpose of this study was to investigate changes in vascularization of the SSP muscle and the relationship to intramuscular fat accumulation following SSP tendon detachment with or without reattachment. One hundred and six rabbits underwent SSP tendon detachment. In groups of ten, thirty rabbits were sacrificed 4, 8, and 12 weeks following detachment. Forty rabbits underwent detachment and immediate reattachment and were sacrificed in groups of ten following 0, 1, 2, and 6 weeks of healing. In groups of twelve, the remaining thirty-six rabbits underwent SSP tendon reattachment 4, 8, and 12 weeks after detachment and were sacrificed 12 weeks later. Vascularization was quantified in each specimen using CD31 immunohistochemistry. Four weeks after SSP tendon detachment, there was an increase in vascularization of the distal SSP muscle that reached significance after 12 weeks of detachment ($p=0.024$). We found that vascularization was positively correlated with intramuscular fat accumulation after detachment only ($r=0.29$; $p=0.008$). After SSP tendon reattachment, immediate or delayed, the correlation between vascularization and intramuscular fat accumulation was not observed. Microscopically, some SSP muscle vascular structures in the reattachment group had thicker vascular walls which were further quantified using αSMA immunohistochemistry. The delayed reattachment group showed an increase in vascular wall thickness in the distal portion of the SSP muscle at 4+12 ($p=0.012$) and 12+12 ($p=0.012$) weeks and in the proximal portion at 4+12 ($p=0.024$) weeks. Further investigation is required to demonstrate a cause/effect relationship between increased vascularization and intramuscular fat accumulation in the context of rotator cuff tear and success of surgical repair.

ACKNOWLEDGEMENTS

First, I would like to thank my thesis supervisor Dr. Odette Laneuville for her mentorship, support, and endless patience.

My thesis advisory committee Dr. Tuan Bui and Dr. Emily Standen.

My thesis examination committee Dr. Marie-Andrée Akimenko, Dr. Tuan Bui, and Dr. Emily Standen.

The members of The Bone and Joint Research Laboratory: Dr. Hans Uhthoff, Dr. Guy Trudel, Dr. Mark Campbell, and Katherine Reilly for support, motivation, and assistance throughout my degree.

Haodong Zhou for being a sounding-board for all ideas, editing material throughout this degree, and for being a fresh perspective when needed.

To my parents and siblings for unfailing support and encouragement to pursue and complete this degree.

Finally, to Isabella Croft Richmond for being supportive of every aspect of the completion of this thesis from beginning to end.

Funding for my graduate studies was provided by the University of Ottawa and the Hans K. Uhthoff FRCSC Graduate Fellowship.

Funding for the project was provided by grants from Workplace Safety and Insurance Board and Canadian Institutes of Health Research awarded to Dr. Odette Laneuville and Dr. Guy Trudel.

TABLE OF CONTENTS

LIST OF FIGURES

LIST OF TABLES

LIST OF ABBREVIATIONS

ADI	architectural difference index
αSMA	alpha smooth muscle actin
CD31	cluster of differentiation 31
FAP	fibro-adipogenic progenitor cell
FOV	field of view
MRI	magnetic resonance imaging
SC	satellite cell
SSP	supraspinatus
VEGF	vascular endothelial growth factor

1.0 Introduction

1.1 Muscle of the Shoulder: The Rotator Cuff

Movement of the shoulder joint, also known as the glenohumeral joint, results from the activity of the rotator cuff; a group of muscles and tendons that provide strength and mobility[1,2]. The glenohumeral joint is a 'ball-and-socket' joint where the humeral head fits into a shallow depression on the scapula; the glenoid fossa[3]. The rotator cuff is responsible for shoulder stability and mobility: abduction, adduction, internal and external rotation of the arm[4]. Skeletal muscles have unique origin and insertion points into bones[3]. The gross anatomy of a skeletal muscle attachment to bone is shown in Figure 1.1. The transition of a skeletal muscle into tendon, the enthesis, and then bone creates a strong attachment and is designed to optimize the transfer of forces from muscle to bone and create movement[5–7]. The rotator cuff is a functional anatomical unit composed of four muscles merging into a tendinous 'cuff' that inserts into the humeral head providing strength and stability during motion of the shoulder[1,7]. Movements of the arm are mediated by the four muscles that make up the rotator cuff; the subscapularis, the supraspinatus (SSP), the infraspinatus, and the teres minor as shown in Figure 1.2[1,8].

Each muscle in the rotator cuff contributes to the specific movements of the shoulder while stabilizing the three bones of the shoulder: scapula, clavicle and humerus[1,9]. The subscapularis is responsible for internal rotation of the humeral head and also prevents dislocation while the arm is raised by pulling the humeral head forward and down[1,9]. The SSP muscle assists the deltoid, a muscle attached to the humerus, and abducts the humerus to a 90º angle[1,8,9]. The SSP muscle is also involved in the movement of the shoulder from 90º to 180º by laterally pulling the humeral head into the shallow glenoid fossa while allowing the deltoid to continue lifting the humerus[1,8]. The main function of the SSP muscle is to prevent dislocation of

the humeral head during overhead reaching and does not significantly contribute to force production for movement of the humerus. The infraspinatus is responsible for the external rotation and backward movement of the humerus and is often assisted by the teres minor and the deltoid[1]. Finally, the teres minor is responsible for assisting the infraspinatus in external rotation as well as transverse abduction and extension[1]. Overall, the function of the four muscles of the rotator cuff is to mediate shoulder movement and maintain stability of the shoulder joint.

The muscles of the rotator cuff provide the force to create movement of the glenohumeral joint while the tendinous attachments to bone translate the tensile forces from muscle to bone[10]. The highly-organized collagen structure of tendons allows for resisting high tensile forces while transmitting forces efficiently[11]. Tendons can have one or two functions; positional and energy storage[7]. All tendons perform positional roles enabling muscles to move bones and positioning the body[5,7]. Few tendons have energy storage capacity and the Achilles tendon is a well characterized example[12,13]. When loaded, the Achilles tendon is able to stretch and store energy which can later be released for the propulsion of the foot from the ground[12]. The Achilles tendon attaches the plantaris, gastrocnemius and soleus muscles to the calcaneous bone in the foot[13,14]. The thick structure of the Achilles tendon provides for both elasticity and shock-absorbance and is involved in supporting tensional forces and producing movement of the foot[12–14]. Tendons with energy storage capacity have higher extensibility, are less stiff and are subjected to small strains compared to positional tendons[12,13]. The tendon structure is optimized to provide appropriate mechanical function across tendon types.

Tendons are composed of a dense fibrous connective tissue rich in collagen[7]. The collagen fibrils are grouped into fibers, fascicles and finally the whole tendon[7,15]. Interspersed between the collagen units throughout the tendon hierarchy is a variety of other non-collagenous

matrix components such as elastin and proteoglycans[5,7]. The extracellular matrix of the tendon accounts for 60 to 85% of the dry weight of the tissue[7,15]. Type 1 collagen is the predominant type and is the principle tensile element of the tendon[7,15]. Tendon cells, the tenocytes, are embedded in an extracellular matrix rich in collagen[16]. How the non-collagen matrix components give tendon its unique properties are less understood. Proteoglycans increase the water content of tendons providing resistance to compression and account for approximately 0.5% of the dry weight of tendons[17]. Although tendons are less metabolically active than associated muscles, tenocytes adapt and remodel in response to mechanical loading while also responsible for the synthesis and turnover of collagen and other molecules of the extra cellular matrix of the tendon[17].

In humans, each muscle of the rotator cuff transitions into tendon before inserting into the humeral head at well-defined insertion sites[1]. Between the tendon and bone, a very small (~0.6 mm) transition zone is visible by microscopy: the enthesis[2]. The enthesis is specialized connective tissue made up of four distinct zones; tendon proper, unmineralized fibrocartilage, mineralized fibrocartilage, and bone[2,18,19]. The enthesis is susceptible to rupture when excessive movements and forces are applied. The composition and organization of the four zones of the enthesis transitions from soft tissue, the tendon, to hard and calcified bone tissue[2,18,19]. In between those two different tissues, the fibrocartilage is present with two very different extracellular matrices: mineralized and unmineralized[2]. The unmineralized fibrocartilage protects the tendon from harmful compression while the mineralized fibrocartilage prevents shearing forces from damaging the insertion into the humeral head[2,18]. The enthesis is specifically structured to withstand the varying directional forces that facilitate the wide range of motion of the glenohumeral joint[2,18]. Rotator cuff tears commonly occur in the SSP tendon prior

to insertion into the humeral head at the enthesis[20–22]. Tears can be partial and progress to a complete detachment of the SSP tendon[21–23]. The distal tendon of the SSP and infraspinatus tendon are often the sites where rotator cuffs tears are diagnosed by medical imaging and observed in individuals performing overhead movements[24–28].

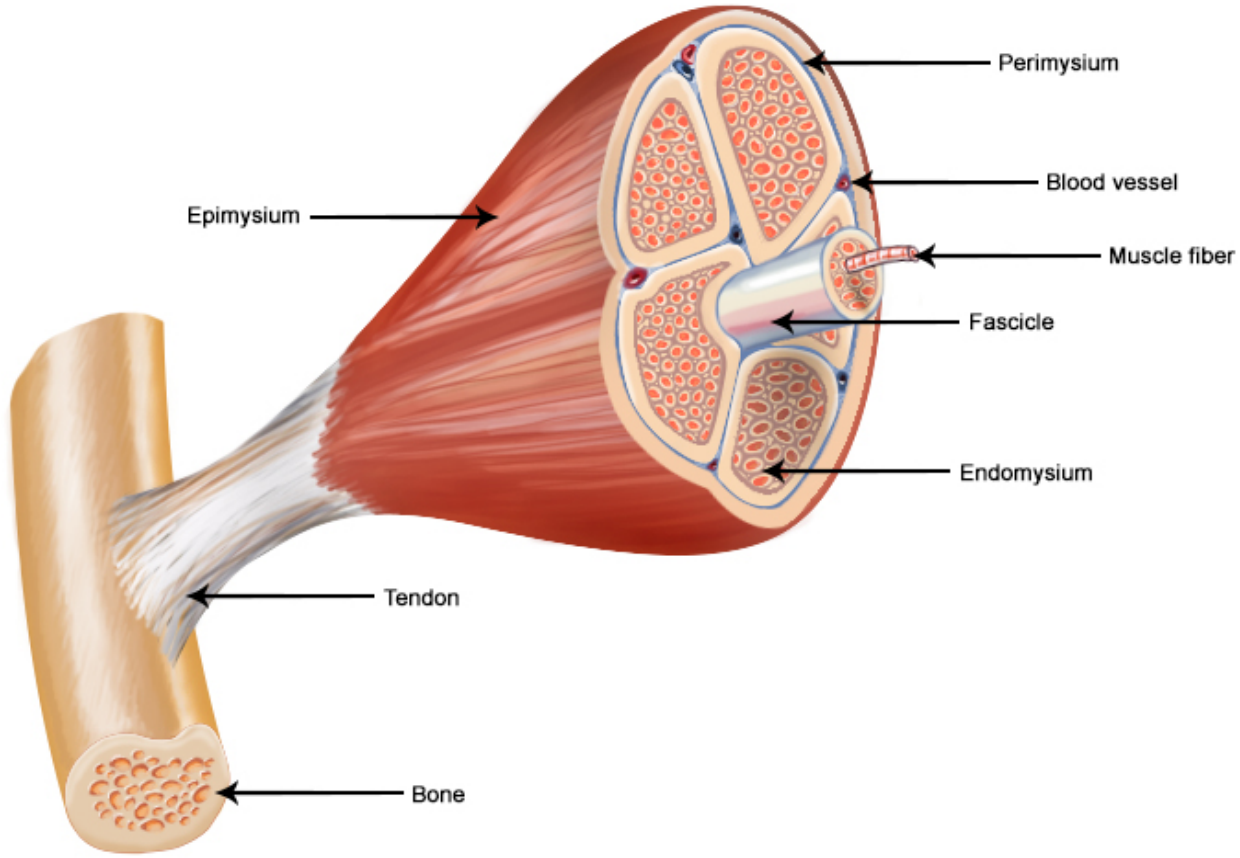

Figure 1.1. The anatomy of a skeletal muscle. A depiction of the attachment of a healthy skeletal muscle to bone. The muscle portion of the musculotendinous unit transitions into tendon which attaches to the bone via the enthesis. The small units that make up a skeletal muscle are also shown: individual muscle fibers are surrounded by endomysium to make up muscle fascicles which are encased in perimysium. Skeletal muscles include muscle fascicles surrounded by epimysium. Vascularization is interspersed between muscle fascicles. Image had been modified from the National Cancer Institute SEER Training Modules[29].

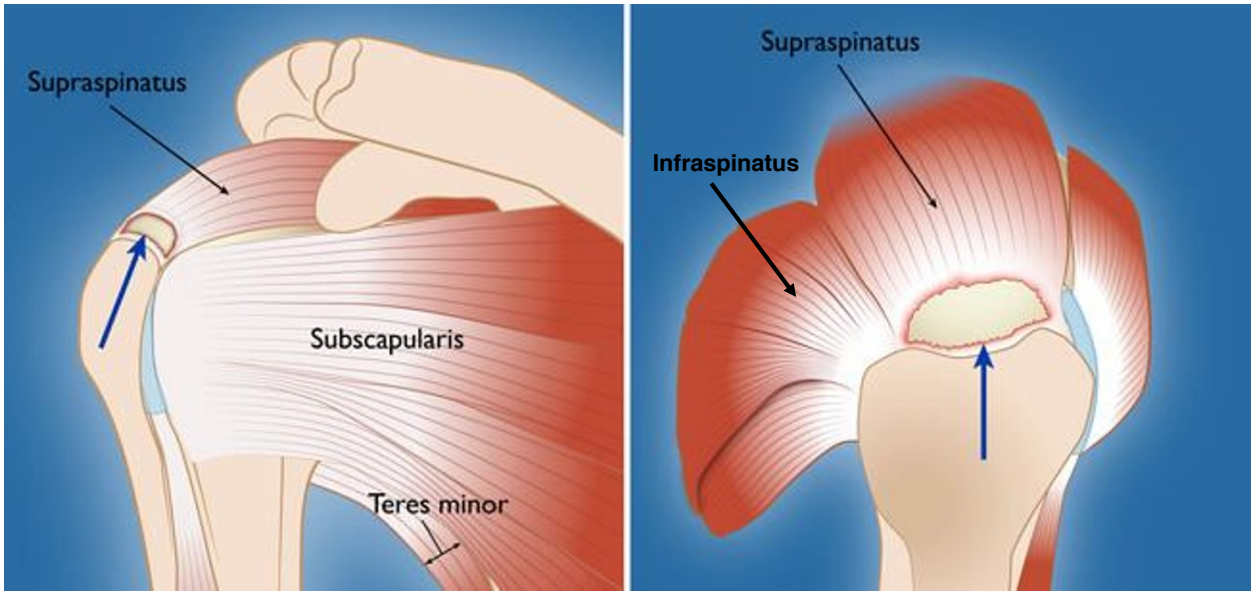

Figure 1.2. The anatomy of the human rotator cuff. Anterior (left) and sagittal (right) views of the right shoulder shows how the muscles of the rotator cuff merge to insert into the humerus and to provide stability of the glenohumeral joint in humans. All four muscles of the rotator cuff, subscapularis, SSP, infraspinatus, and teres minor, the associated tendons and insertion points into the humeral head are shown. The location of common rotator cuff tears is indicated by blue arrows at the insertion of the SSP tendon. Image has been modified from The American Academy of Orthopaedic Surgeons[30].

1.2 Rotator Cuff Tears

Rotator cuff tears are a significant clinical problem affecting ~35% of individuals over 60 years of age[31]. The SSP tendon at the distal insertion into the humeral head is the most commonly torn tendon as shown in Figure 1.2[24–28]. The proximal insertion of the SSP tendon into the supraspinous fossa of the scapula is rarely torn since it is not involved in stabilizing the shoulder joint[1]. A tendon tear often results from repetitive overhead reaching with weights[28,31]. In humans, SSP tendon tears may begin as small, or partial tears, and progress over time to become full complete tears[21]. Occasionally, SSP tendons will tear completely and the distal end of the SSP muscle will no longer be attached to the humeral head[21,28,32]. If untreated, a detached tendon is challenging to surgically repair because the tendon will degenerate and the unused muscle will atrophy and retract[28,33]. Partial tears fail to heal without surgical intervention in 20 to 95% of the cases depending on individual patient characteristics including: age of patient, severity of tendon tear, and length of time the tendon has been torn, making them difficult to treat[34,35]. The longer the duration after a tendon tear, the more significant the complications are, decreasing the likelihood of a successful surgical reattachment. The low rate of spontaneous healing justifies the need for surgical interventions to restore normal shoulder function early after injury[7,31]. Partial tears often lead to a slower progression of tendon degeneration when compared to complete tears where the functional structure and alignment of tenocytes will slowly degrade while the density of adipose tissue and vascularization will increase in the tendon[31,36]. Tendon degeneration further prevents successful surgical reattachment as the structural integrity of the tendon is lost and cannot be successfully reattached to the bone.

Following a rotator cuff tear patients can experience a wide range of symptoms. Shoulder pain and reduced range of motion observed at physical examination often accompany the rotator

cuff tear although some individuals have asymptomatic tears[37–39]. One study evaluated 411 asymptomatic individuals to determine the prevalence of asymptomatic rotator cuff tears and found that 23.4% of individuals had a rotator cuff tear despite not exhibiting any diagnostic characteristics[39]. A second study evaluated the degree of degeneration of rotator cuff tendons in cadavers and quantified the level of degeneration and presence of partial tears[38]. Sano et al., found 17 out of 76 cadaveric shoulders had a partial rotator cuff tears and showed significant signs to degeneration; fiber thinning, tissue granulation, and fiber tearing, when compared to intact tendons[38]. In addition to shoulder examination, medical imaging provides information about the extent and location of the tendon tear and about muscle condition: including size (retraction, atrophy) and composition (intra- and extramuscular fat accumulation)[28,37,40–42]. Symptoms, clinical assessment, and imaging results in the diagnosis of rotator cuff tear are often correlated[43,44]. In the case of a complete tear of the distal end of the SSP tendon, the shoulders ability to abduct the humerus will be prevented and symptomatic[45]. The muscular changes, particularly fat accumulation in the muscle, compound rotator cuff tears and contribute to low surgical success rates[44,46,47]. A recent study found that re-tear rates following surgical repair were correlated with age and size of the tendon tear[48]. Individuals less than 50 years old had a re-tear rate of 5% 6 months following surgical repair. The re-tear rate increased to 34% in individuals over 80 years old[48].

Fat accumulation in the SSP muscle is a criterion frequently used as a prognostic factor to determine a patients' eligibility for surgical repair. Using magnetic resonance imaging (MRI), fat accumulation is scored on the Goutallier scale, a semi-quantitative assessment, with a score of 0 to 4 with 4 as the highest score[25,49,50]. The Goutallier scale alone provides limited information mainly because of the low inter-observer reliability and the lack of evaluation of the importance

of tear as a whole[24]. Currently, the Goutallier score is used in association with the clinical assessment and visualization of the tear by medical imaging to guide the decision to surgically repair a torn tendon[24]. The rationale of using the Goutallier in the clinical decision is supported by the results from epidemiological studies. Intramuscular fat accumulation in rotator cuff tears has been shown to have a strong association with negative surgical outcomes[25,44,46,47,49–51]. In the SSP muscle, fat starts accumulating early in and around the muscle, progresses over time, and is not reversed following surgical reattachment[26,51,52]. A detachment in the SSP tendon can also cause fat accumulation in the adjacent but intact infraspinatus muscle despite maintaining continuity[40]. Intramuscular fat impairs normal muscle functioning by preventing the proper contraction of myocytes and disrupting normal muscle architecture[53–56]. Intramuscular fat is also associated with decreased function of resident satellite cells(SC)[56]. The presence of intramuscular fat is used as a prognostic factor mainly because the presence of high levels of intramuscular fat prevents the proper healing and function of rotator cuff muscles[25,44,46,47,49–51].

There are several different approaches to treating rotator cuff tears and the decision takes into consideration individual patient characteristics such as; severity of tear, duration of tear, impact on quality of life, and age of patient[34]. If a rotator cuff tear does not significantly impact a patients' quality of life, non-operative treatments may be the best course of action[34]. Non-operative treatments primarily focus on physiotherapy for the affected joint to strengthen and minimize the effects of a torn, partial or full-thickness, rotator cuff[34]. Non-operative treatments are also used in patients who are in the waiting period for surgical rotator cuff repairs[34]. The current standard of care for surgical repair is fully arthroscopic surgeries but mini-open repairs are sometimes used[34,57–59]. Arthroscopic surgery is typically a day surgery in which minor skin incisions are made to visualize and repair the torn tendon[57]. These surgical protocols are

minimally invasive, do not require long hospital stays, and decrease the risk of post-operative complications such as infection[57]. Arthroscopic repairs are associated with decreased postoperative pain, less complications, and faster recovery although functional outcomes and re-tear rates remain the same when compared to mini-open repairs[34].

When performing a surgical repair, the arrangement of sutures has been evaluated in association with re-tear. A recent review compared common techniques; single-row, double-row, and tripe-row repairs, to determine if any are associated with superior clinical outcomes[33]. Suture techniques refer to the orientation of the sutures inserted into the humeral head to reattach the SSP tendon. Although most studies indicated that newly developed techniques improve the biomechanical strength of the repair, this was not translated into improved surgical outcomes[33]. Lower tendon re-tear rates are observed when the double row technique (19.5%) was used when compared to the triple row technique (23.5%) and single row technique (30.3%) [33]. Although re-tear rates improved with some surgical techniques, the failure rate of rotator cuff repair remains high[33]. It is difficult to compare between studies when evaluating clinical outcomes primarily because of the inconsistency in the criteria used for surgical success, the duration of the follow-up period, and the classification of the original injury[33,34].

The repair of rotator cuff tears has made many strides toward increasing surgical success rates. In the USA there are approximately 4.5 million annual visits to physicians regarding shoulder pain and discomfort[28,34]. These visits translate into 75,000 surgeries costing approximately $14,000 USD each with mini-open techniques costing approximately $1,000 USD less than arthroscopic techniques[28,57]. Despite development of new techniques, new anchor design, and increasing knowledge of the disease process, the surgical success rate for complete rotator cuff tears remains between 69 and 95% [28,57]. Experimental studies provide valuable

avenues to investigate the biological process of rotator cuff tears, decipher the pathophysiology of rotator cuff tears, and test new surgical interventions.

1.3 Fat Accumulation in Skeletal Muscle

Both skeletal muscle and bone come from the same mesodermal embryonic origin and maintain their functional structure though active loading[60]. When bones and muscles are not loaded within natural capacity, they will undergo physiological changes that affect their function and composition[61]. In skeletal muscle, intramuscular fat accumulation can be problematic for the contractile ability of the muscle because it alters the composition and arrangement of myocytes[61]. Intramuscular fat accumulation has been studied in the context of optimization of intramuscular fat content in the meat industry. In the beef industry, intramuscular fat is referred to as marbling in steaks and represents an important characteristic to optimize quality and taste of the meat[62]. Specific breeds of livestock, such as Wagyu cattle, have an optimal intramuscular fat content[62]. Aside from the genetic contribution to marbling in livestock, the energy derived from the diet is altered to modify the intramuscular fat content[62]. Similarly, humans can be subject to increase intramuscular fat density if they are consuming a high calorie diet over an extended period of time[61,63]. Increased intramuscular fat content has also been linked with aging. As humans age, there is a net loss of skeletal myocytes and an increase in adipose tissue, both causing a loss in strength of the muscle[61]. It is unknown if muscle force production is primarily affected my muscle atrophy, fat accumulation, or a combination of both. By identifying the pathways and contributors to intramuscular fat accumulation, therapies could be developed to reduce the harmful effects of intramuscular fat on muscle function in human.

It has been shown that progenitor cells resident in healthy skeletal muscle can contribute to intramuscular fat accumulation. Progenitor cells include fibro-adipogenic progenitor cells

(FAP), SCs, and pericytes. FAPs and pericytes are found in close association with vascularization in skeletal muscles[55,64,65]. In response to muscle injury Type 1 pericytes become committed to an adipogenic differentiation pathway and potentially contribute to fat accumulation[64,66]. FAPs also respond to muscle injury by differentiating into skeletal muscle adipocytes but, in the presence of efficient skeletal myocyte regeneration, FAPs will return to their dormant state[55,67]. Both potential sources of adipocytes can cause an increase in intramuscular fat and a decrease in myocyte proportion in skeletal muscle with changes in the fundamental architecture of the muscle preventing proper contraction[65,67]. In the aging population, the increased intramuscular fat content is directly related to a decreased force production by the skeletal muscle[47,53]. No effective treatments directly address the combined intramuscular fat content, weakening of skeletal muscle, and increased risk of injury. Intramuscular fat accumulation can be prevented by resistance training and aerobic exercise but will not prevent fat accumulation in response to injury[60]. When investigating degenerative myopathies, low intensity, high frequency vibrations have been shown to decrease fat depots in mice[68]. High frequency vibrations can mimic low intensity, long duration exercise which is associated with decreased intramuscular fat accumulation in skeletal muscles[68]. One study by Davis et al., attempted to maintain muscle strength despite intramuscular fat accumulation in response to injury and found that statin treatment can have a protective effect on muscle atrophy[32]. Statins inhibit the synthesis of precursor enzymes for cholesterol and are involved in triggering the inflammatory signalling pathways[32]. Attempts at reversing intramuscular fat accumulation in animal models of after rotator tear have not been successful.

In the clinical context of rotator cuff tears, fat accumulation associated with rotator cuff tears has been shown to occur early, to persist over time, and to be associated with re-tearing of

the tendon following surgical repair. Gladstone et al., have suggested a 'point of no return' for intramuscular fat accumulation in rotator cuff tears where the fat accumulation will prevent any surgical repair attempts from being successful[44]. In a study evaluating surgical outcomes at a one year follow-up, 70% of individuals who had moderate to severe fat accumulation experienced a re-tear while only 29% of individuals with no or mild fat accumulation experienced a re-tear[44]. Using a regression analysis, Gladstone et al., confirmed previously reported semi-qualitative data and fat accumulation was identified as an independent factor that predicts functional outcomes following rotator cuff repair[44]. In an attempt to characterize the origin of adipocytes, Klomps et al., used a transgenic GFP mouse line to determine if bone marrow derived adipocytes contributed to intramuscular fat accumulation and found that less than 10% of adipocytes found in the muscle originated from bone marrow[69]. Despite extensive characterization of intramuscular fat in rotator cuff tears, there is little information about the origin of the adipocytes limiting the ability for treatment and reversal of fat accumulation in the muscle.

1.4 Animal Models of Rotator Cuff Tear

The rotator cuff is a musculoskeletal feature that is unique to higher primates and humans. A true rotator cuff forms by the fusion of the SSP and infraspinatus tendons prior to insertion into the humeral head[70,71]. Mammals have four muscles and tendons of the rotator cuff but the tendons do not merge prior to insertion into the humeral head[3,35,71]. The structure of a true rotator cuff is associated with the increased range of motion in the forelimbs of bipedal mammals, specifically the ability to reach overhead[71]. The biology of rotator cuff tears is commonly studied using the mouse, rabbit, sheep, and pig models that exhibit a different organization of the rotator cuff and more limited shoulder movement. Although the rotator cuff

of animal models used for research differs from human anatomy, valuable information can be derived to understand how the shoulder structure allows for movement.

Animal models allow for control of variables potentially contributing to rotator cuff tears. In particular, the size and location of the tear and timing of the repair surgery can be reproduced consistently in animals[35]. The changes in the different tissues can be monitored precisely over time and examined using imaging techniques similar to what is used in clinic. Tissues are available for histology analysis providing details at the cellular and molecular level. By using an animal model, variables influencing the tear, the changes associated with rotator cuff tears including tendon dehiscence, muscle atrophy, muscle retraction, and intra- and extra-muscular fat accumulation and biomechanical properties can all be measured consistently.

Different model animals have been described in the literature and used for the study of rotator cuff tears each with advantages and limitations. A comparative analysis of rotator cuff tear models has divided commonly used animal models into three groups; small animals, large animals, and primates. Ten species were categorized into these three groups and comparisons of rotator cuff muscle were reported using an architectural difference index (ADI) described by the authors[71]. The ADI score was used as an indication of how similar one species is to another when comparing the 4 rotator cuff muscles; the lower the score the greater the similarity to the human muscle characteristics[71]. In the study by Mathewson et al., ADI is the combination of fiber length-to-moment arm ratio, fiber length-to-muscle length, and the fraction of the total rotator cuff physiological cross-sectional area[71]. How an animal uses the muscle for specific functions changes the size and force production of the muscles of the rotator cuff. When pooling architectural characteristics of the rotator cuff muscles, the authors concluded that non-human primates were the most similar based on ADI scores, followed by small mammals including

mouse, rat, and rabbit[71]. The least similar animals were the large mammals and differences were attributed to gait which changes the structure and function of the rotator cuff compared to the shoulder joint in humans[71].

Our laboratory has previously characterized the rabbit model of rotator cuff tear and this project is an extension of previous work[26,51,52,72]. The advantages and limitations of the rabbit model for the study of the rotator cuff tear are described below. Rabbits have the same four shoulder muscles as humans although they are not in an identical orientation[71]. When combining all four muscles of the rotator cuff, the rabbit ADI score equaled approximately 5, was in the mid-range of similarity, but when further broken down into individual muscles, the rabbit SSP muscle ADI score was approximately 2 indicating a high similarity between the rabbit and human SSP muscles[71]. The rabbit is a large enough animal to reproduce the standard-of-care surgical techniques used in humans[7,72]. Rabbits also demonstrate a similar progression of deterioration of the SSP muscle following a complete distal SSP tendon tear including the development of atrophy, retraction, and fat accumulation[7]. The persistence of fat accumulation following SSP tendon reattachment mimics the clinical presentation of fat accumulation in humans[26,51,72]. These characteristics are not consistently observed in all animal models, such as the sheep model. Although the rabbit rotator cuff tear model presents advantages, some limitations were noted. First, when a tendon is detached in a healthy rabbit, no degeneration or disease is present as often observed in humans[35]. Tendon dehiscence refers to a tendon degenerated and diseased with ruptures induced by stretching performed at the reattachment surgery and commonly observed in humans who have experienced a long duration of tendon tear[35]. Second, rabbits are quadrupeds and have limited overhead reaching ability[71]. As such, the rabbit shoulder is loaded in the rabbit model while human shoulder is not an inherently loaded

joint[35,71]. Third, the SSP and infraspinatus tendons do not merge together prior to insertion into the humeral head as we observe in humans so a true rotator 'cuff' structure is not present[35,71]. Finally, rabbits have a different bony anatomy of the shoulder when compared to humans. Rabbit acromion is inferior to the SSP tendon and partially covers the infraspinatus and teres minor opposed to the acromion being directly superior to the SSP tendon[35]. In humans, the acromion is superior to the SSP tendon and can be associated with wearing and partial tears of the SSP tendon[35].

1.5 Previously Published Work

The Bone and Joint Research Laboratory has previously published data using the rabbit model of rotator cuff tear contributing knowledge of the biological process of rotator cuff tears and surgical reattachment. Three separate protocols; detachment, detachment and immediate reattachment, and detachment and delayed reattachment, have been used to characterize SSP muscle changes including fat accumulation and muscle atrophy[26,51,72]. In the detachment only protocol, significant fat accumulation was measured and observed both intramuscularly and extramuscularly[26]. Increased fat was noticeable as early as 4 weeks following SSP detachment[26]. Fat accumulation continued to progress through to the last time point; 12 weeks[26]. Using MRI, authors reported quantitative data (as opposed to using the semi-quantitative Goutallier scale) and the extramuscular fat accumulation was three times greater than intramuscular fat accumulation[26]. Interestingly, the intramuscular fat accumulation followed an increasing proximal-to-distal gradient where the highest density of fat accumulation was distal and closest to the detachment site[26]. Intramuscular fat accumulation and muscle atrophy occur simultaneously and must be taken into account when assessing muscle volume as fat accumulation can mask decreased volume of myocytes[26].

The repair protocols were designed to determine the effect of the timing of the repair surgery after a complete tear. Muscle changes occurring in the SSP muscle following delayed and immediate surgical reattachment have been reported using computed tomography scans and histology methods. The SSP tendon detachment and immediate reattachment protocol also assessed how SSP muscle retraction, a consequence of complete SSP tendon tears, contributed to changes in the SSP muscle. The SSP muscle lost significant volume due to atrophy up to 2 weeks following immediate reattachment but had recovered after 6 weeks[72]. Intramuscular fat accumulation was consistently higher in the experimental group and became significant 1 week after surgical reattachment in the mid portion of the SSP muscle and significant in the whole SSP muscle after 6 weeks[72]. The intramuscular fat accumulation followed the same accumulation gradient where the highest density of intramuscular fat was measured closest to the tendon tear[72]. In the delayed reattachment group, the repair surgery was completed at various times after detachment and allowed a 12-week period of healing before harvesting. Both intra and extra-muscular fat accumulation followed the increasing proximal-to-distal gradient as previously observed in the detachment only group and surgical repair did not reverse fat accumulation[51]. A progression in muscle atrophy was observed over time following delayed reattachment[51].

The main findings from the rabbit model of rotator cuff tear include intramuscular fat accumulation within the SSP muscle and localized to the distal region closest to the tendon tear[26,51,72]. Intramuscular fat is present 1 week following detachment in the absence of muscle retraction, persisted after immediate and delayed reattachment[52,72]. A successful reattachment of the SSP tendon did not reverse the fat accumulation[51,72]. Fat accumulation is currently used as a prognostic factor to establish a patients' eligibility for surgical repair but the pathophysiology of intramuscular fat accumulation is largely unknown. Elucidating the origin of this accumulation

may provide avenues to improve surgical repair and functional outcomes following SSP tendon tear.

1.6 Vascularization of the Skeletal Muscle

The vascularization of skeletal muscles is important for nourishing the muscle and eliminating metabolic waste[73]. The blood supply adapts during exercise, growth, development, and healing in response to metabolic requirements[74]. Vascularization is organized to allow for the transport and exchange of gas and solutes in various tissues including skeletal muscle[74]. From the heart, oxygenated blood is pumped through large arteries around the body[75]. These large arteries have a thick muscular layer and contribute to the active pumping of blood throughout the body[75]. As the vascularization is reaching the point where molecules are exchanged across its surface, the vascular wall begins to thin forming smaller arterioles[75]. These arterioles still contribute to the pumping of blood throughout the body but are much smaller in diameter[75]. The smallest form of vascular structure are capillaries which are divided into three distinct types: fenestrated, sinusoidal, and continuous[75,76]. Capillaries are very small in diameter and only consist of a basement membrane, endothelial cells, and pores which allow for the exchange of solutes and gases across the endothelial wall[74,75]. Moving blood back toward the heart, the veins will begin increasing in diameter but have a thinner smooth muscle cell layers when compared to arteries[75]. Vascularization is composed of three distinct layers of cells; tunica intima, tunica media, and tunica externa as shown in Figure 1.3[74,75]. The tunica intima is the inner most layer of vascularization and is composed of endothelium and an internal elastic membrane[74,75]. The middle layer, tunica media, is the thickest and most variable layer of vascularization as it is composed of elastic fibers, connective tissue, and vascular smooth muscle cells[74,75]. Arteries have a larger smooth muscle layer compared to veins because they participate

in active pumping to blood throughout the body[74,75]. Finally, the outermost layer, the tunica externa is made up of connective tissue with nerves and is separated from the tunica media by the external basement membrane[74,75]. The tunica intima is the least variable component of vascularization, consisting in endothelial cells and present in all types of vascularization[74,75]. The tunica media and tunica externa varies in thickness due to changing smooth muscle composition depending on the location, size, and function of the blood vessel[74,75].

The SSP muscle is principally vascularized by the suprascapular artery entering in the midsection of the muscle belly as shown in Figure 1.4[77]. Two main branches of the suprascapular artery diverge at the entry point into the muscle and migrate towards the distal and proximal ends of the SSP muscle[74,77]. These large branches further divide into arterioles and capillaries to vascularize individual muscle fibers[74]. The SSP tendon is vascularized by the acromial branch of the thoracoacromial artery with contribution from the suprascapular artery[78,79].

Muscle structure changes occurring after rotator cuff tears are significant and attributed to muscle disuse. While muscle atrophy can be reversed by exercise, fat accumulation is persistent and does not reduce following surgical reattachment[72]. SSP tendon changes are not well understood and an increase in the vascularization of the SSP tendon following a rotator cuff tear was previously documented in association with the degeneration of the tendon[80]. Longo et al., conducted a study using samples from individuals who underwent arthroscopic repair of the SSP tendon to determine any cellular changes occurring in the tendon following a tear[80]. They found that there was an association between increased vascularity and level of tendon degeneration[80]. The changes in the vascularization of the SSP muscle in association with rotator cuff tears remain to be characterized. The rationale for describing the changes of the SSP vascular structures is to further understand the origin of adipocytes accumulating after rotator cuff tear.

Intramuscular fat accumulation has previously been observed with ageing, insulin resistance, metabolic, orthopaedic, and some neurologic conditions such as Duchenne muscular dystrophy and the potential contribution of vascularization to fat accumulation remains uncharacterized in those pathologies[60,68].

Vascularization has been associated with the development and proliferation of adipose tissue in the subcutaneous fat depot[63,81]. The most studied fat depots in the body include subcutaneous, visceral, and muscular, each with specific structural characteristics and dynamic changes associated with pathologies[81]. It has been hypothesized that adipocytes have specific autonomous functions that are not reliant on the depot they are placed in[82]. The subcutaneous depot is the most characterized and is associated with protective functions within the body such as heat retention[81,82]. Subcutaneous adipose tissue expansion is reliant on vascularization for growth and proliferation; both associated with a higher demand for oxygen and circulating fatty acids, and endocrine function[81,82]. Much remains to be understood about intramuscular fat depot and the mechanisms of expansion of adipose tissue.

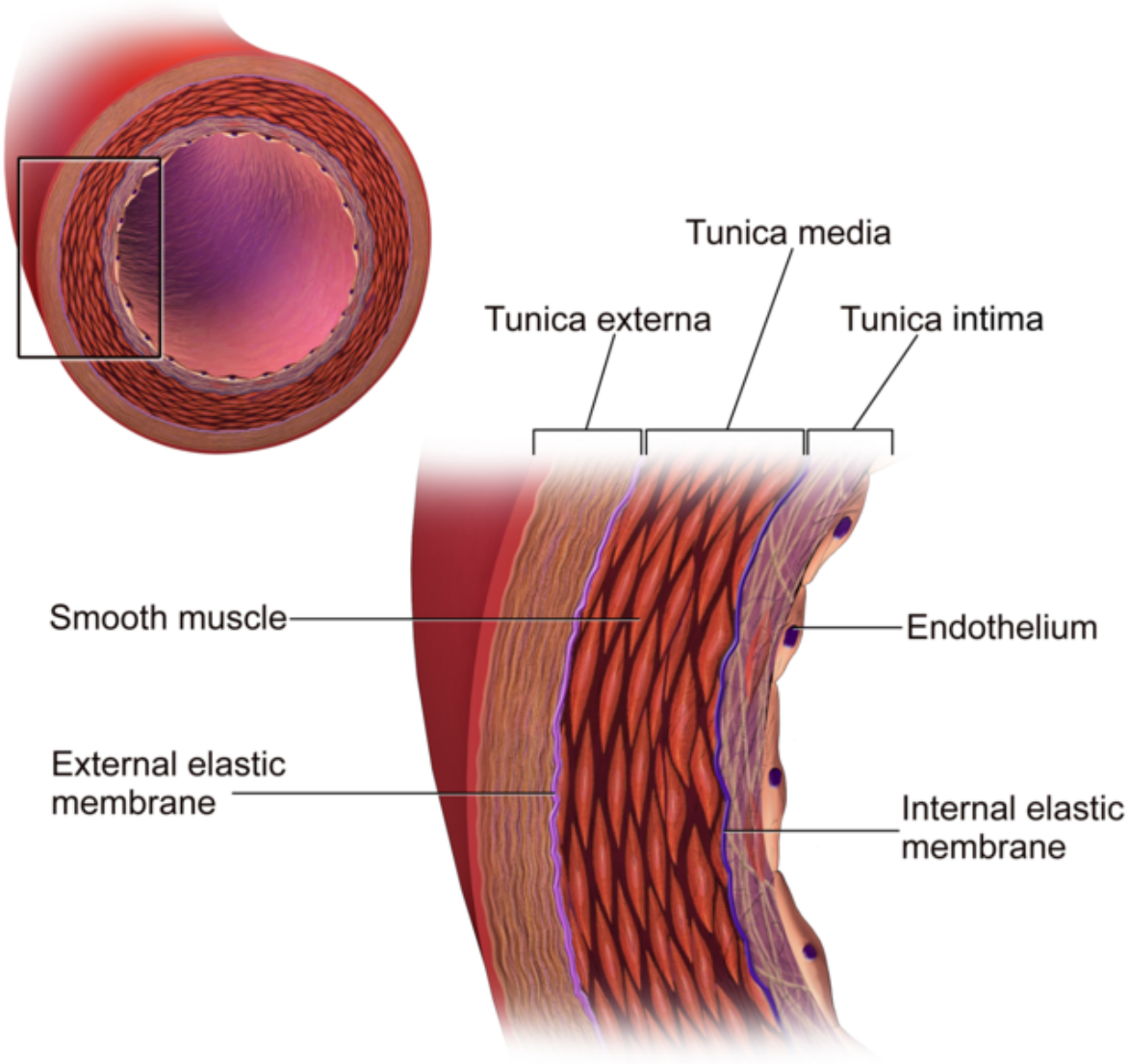

Figure 1.3. Structure of vascularization. Transverse depiction of a large blood vessel showing the composition of the three major layers of vascular tissue; tunica intima, tunica media, and tunica externa. The thickness of the tunica externa and tunica media will vary depending on blood vessel diameter and function while the tunica intima containing the vascular endothelium, a monolayer of endothelial cells, is present in all sizes of vascularization. Schematic is from lumencandela: Blood Vessel Structure and Function[83].

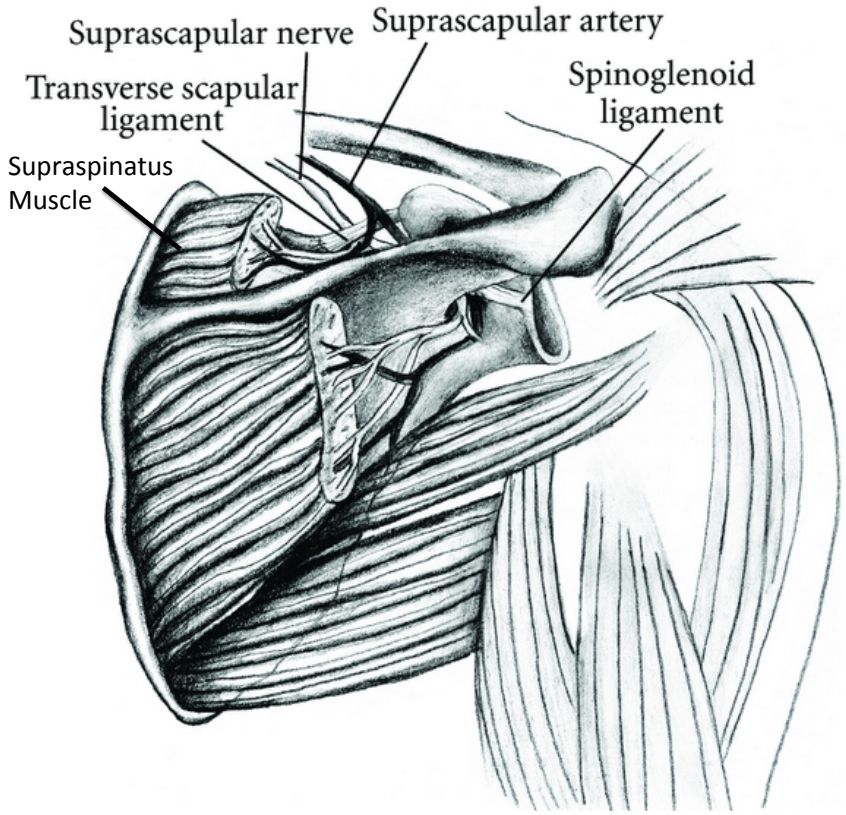

Figure 1.4. Vascularization of the human SSP muscle. An anterior view of the left shoulder is shown. The suprascapular artery enters the middle portion of SSP muscle and diverges in two main branches to provide the blood supply to the entirety of the muscle. This figure was modified from 'Suprascapular neuropathy'[84].

1.7 Purpose, Objectives, and Hypotheses

The purpose of this study is to provide insight into the pathophysiology of intramuscular fat accumulation of the SSP muscle after rotator cuff tear with and without surgical reattachment. I investigated the structural changes of vascularization in the SSP muscle and correlated those with previously collected intramuscular fat data from the same specimens. The rabbit model of SSP tendon tear with and without surgical reattachment previously characterized in our laboratory was used as a model.

1) The first objective was to quantify the vascularization of the SSP muscle following different durations of SSP tendon detachment with or without reattachment. To detect vascular structures in the SSP muscle, I used immunohistochemistry and an antibody specific for endothelial cells. The number of stained vascular structures was quantified in histology sections from three different surgical groups: SSP detachment, SSP detachment and immediate reattachment, and SSP detachment and delayed reattachment.

   Hypothesis: Vascularization of the SSP muscle will increase following SSP tendon detachment, with or without reattachment and be localized closest to the tendon tear where intramuscular fat was previously documented to accumulate in the SSP muscle.

2) The second objective was to quantify the relationship between vascularization and intramuscular fat accumulation. Intramuscular fat data previously measured provided and only available for two of the three experimental groups: detachment only and detachment and delayed reattachment.

   Hypothesis: Vascularization and intramuscular fat will be positively correlated in the SSP muscle following detachment with or without delayed reattachment.

3) The third objective was to quantify the thickness in vascularization observed in the detachment and delayed reattachment group using αSMA immunohistochemistry
Hypothesis: Thick vascularization will increase following SSP tendon detachment with delayed reattachment and be localized to the distal portion of the SSP muscle closest to the tendon tear.

2.0 Methods

2.1 Source of Samples

The rabbit model of rotator cuff tear has been previously described by The Bone and Joint Research Laboratory[26,51,72,85,86]. After obtaining institutional animal care committee approval (Protocol Number ME-2479) one hundred and fifty-four female New Zealand white rabbits (3.0 kg) were randomly assigned into three experimental groups: SSP tendon detachment (detachment), SSP tendon detachment and immediate reattachment (immediate reattachment), and SSP tendon detachment and delayed reattachment (delayed reattachment). Each group underwent SSP tendon detachment with or without reattachment as described below. Schematic of source of samples is shown in Figure 2.1.

SSP Tendon Detachment

SSP tendons of experimental rabbits were transected from the attachment to the humeral head and any remaining tendon was removed from the insertion site. The SSP tendon stump was wrapped in a polyvinylidene fluoride membrane (5μm, Durapore; Millipore, Bedford, MA, USA) to prevent spontaneous reattachment. The incision site was closed in layers and pain was controlled using transdermal fentanyl applied one day prior to surgery and removed four days following surgical detachment. Buprenorphine, an opioid, was also administered subcutaneously for three days post-operatively. Rabbits were not immobilized, housed individually, and provided free access to food and water.

SSP Tendon Reattachment

SSP tendons were reattached immediately or following 4, 8 or 12 weeks of detachment. Three 1-mm holes were drilled through the lateral aspect of the greater tuberosity and two non-absorbable 3 – 0 prolene sutures were used to reattach the SSP tendon. To control pain,

transdermal fentanyl was applied one day prior to surgery and removed four days following surgical detachment. Buprenorphine was also administered subcutaneously for three days post-operatively. The shoulders were not immobilized and rabbits were housed individually with free access to food and water.

Collection of Specimens

All rabbits were sacrificed using a pentobarbital overdose and both shoulders were harvested en bloc avoiding dissection of the SSP muscle from the scapula or any extramuscular fat. Specimens were frozen at -20ºC until processing. The time points are identified as number of weeks following detachment + number of weeks after surgical reattachment: detachment (4, 8, 12 weeks), immediate reattachment (0, 0+1, 0+2, 0+6 weeks), and delayed reattachment (4+12, 8+12, 12+12 weeks). In each experimental group, the operated shoulders were placed into the experimental groups. Both shoulders from age matched controls were harvested to create the unoperated control group. Frozen SSP muscles were provided for this study and used to investigate the change in SSP muscle vascularization following detachment with or without surgical reattachment.

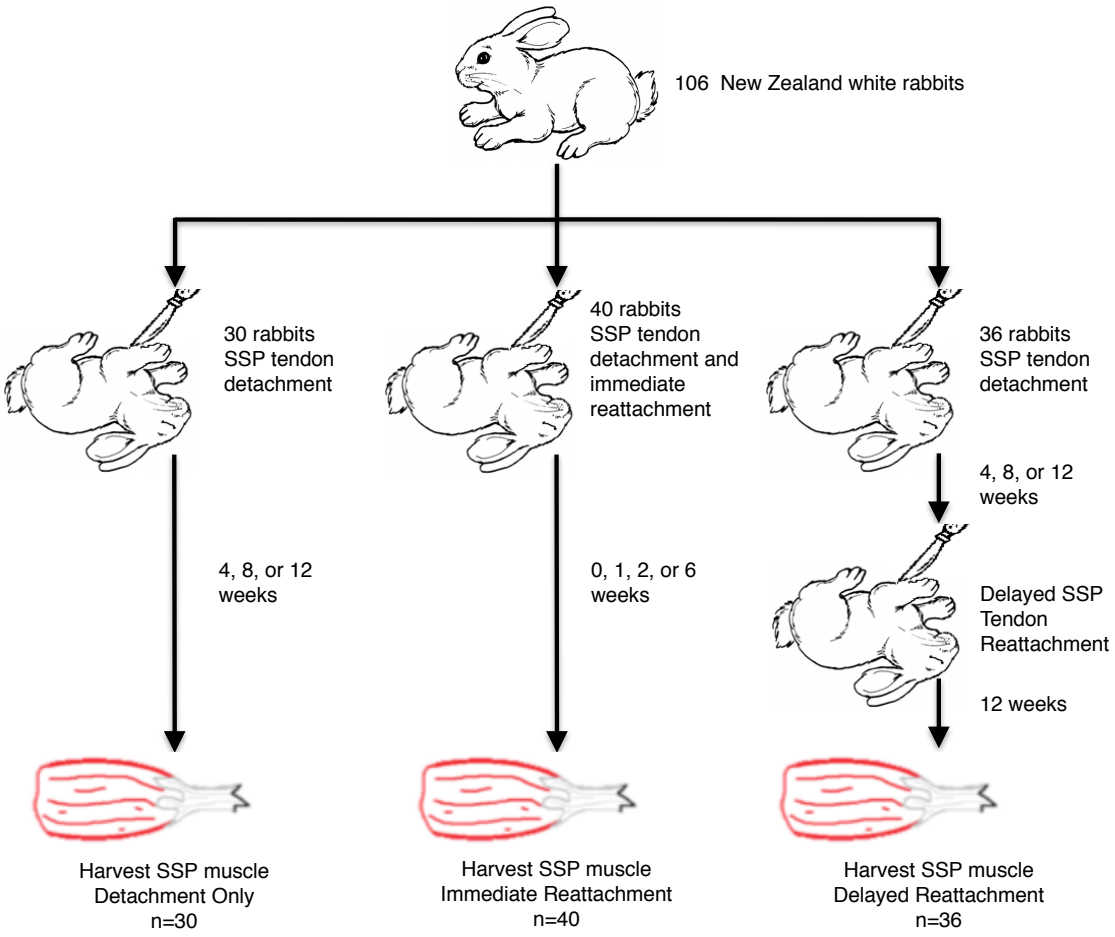

Figure 2.1. Representation of the distribution and surgical protocols for each of the three experimental groups. The detachment only group underwent surgical detachment of the SSP tendon followed by 4, 8, or 12 weeks of healing. The immediate reattachment group underwent SSP tendon detachment and immediate reattachment followed by 0, 1, 2, or 6 weeks of healing. The detachment and delayed reattachment group underwent SSP tendon detachment for 4, 8, or 12 weeks followed by SSP tendon reattachment and 12 weeks of healing. Forty-eight age-matched control rabbits were proportionally distributed to every time-point in each experimental protocol. This portion of the protocol was conducted prior to this study and whole SSP muscles were provided.

2.2 Detachment Group

In the detachment only group, forty-five rabbits were divided into two groups; surgical detachment and controls. Thirty of the rabbits underwent SSP tendon detachment at the distal end near the footprint in alternating shoulders and were harvested in groups of ten after SSP tendon detachment. The groups are indicated as the number of weeks following SSP tendon detachment: 4 weeks, 8 weeks, and 12 weeks. The remaining fifteen rabbits had no surgical intervention and both shoulders were harvested at the same time points to serve as age-matched controls.

2.3 Immediate Reattachment Group

In the immediate reattachment group, fifty-five rabbits were randomly distributed into the surgical and control groups. In the surgical group, forty rabbits were killed in groups of ten at time points indicated as weeks of detachment + weeks after reattachment: 0+0 weeks, 0+1 week, 0+2 weeks, and 0+6 weeks. The remaining fifteen rabbits did not undergo any surgical intervention and both shoulders were harvested in groups of five at the same time points to serve as age-matched controls.

2.4 Delayed Reattachment Group

In the delayed reattachment group, fifty-four rabbits were randomly distributed into the surgical and control groups. In the surgical group, thirty-six rabbits underwent SSP tendon detachment, described above, at the distal end of the SSP tendon and were reattached in groups of twelve at 4, 8, and 12 weeks following detachment. The rabbits from all three groups were killed in groups of twelve, 12 weeks following SSP tendon reattachment. The time points are indicated as weeks of detachment + weeks after reattachment: 4+12 weeks, 8+12 weeks, and 12+12 weeks. The remaining eighteen rabbits did not undergo any surgical intervention and both

shoulders were harvested in groups of six at the same time points to serve as age-matched controls.

2.5 Preparation of Samples

From the collection of frozen SSP muscles, all histology samples were prepared following the same protocol. The SSP muscles were warmed to room temperature where 3 sections of 2-mm thickness were harvested from the distal, middle, and proximal regions. The sections were then fixed in 10% neutral buffered formalin for 48 hours, processed through graded alcohols and embedded in paraffin. 5-μm thick sections were then cut using a microtome (Leica RM2235, Concord, ON, CA) from each paraffin bloc and mounted for immunohistochemistry as shown in Figure 2.2.

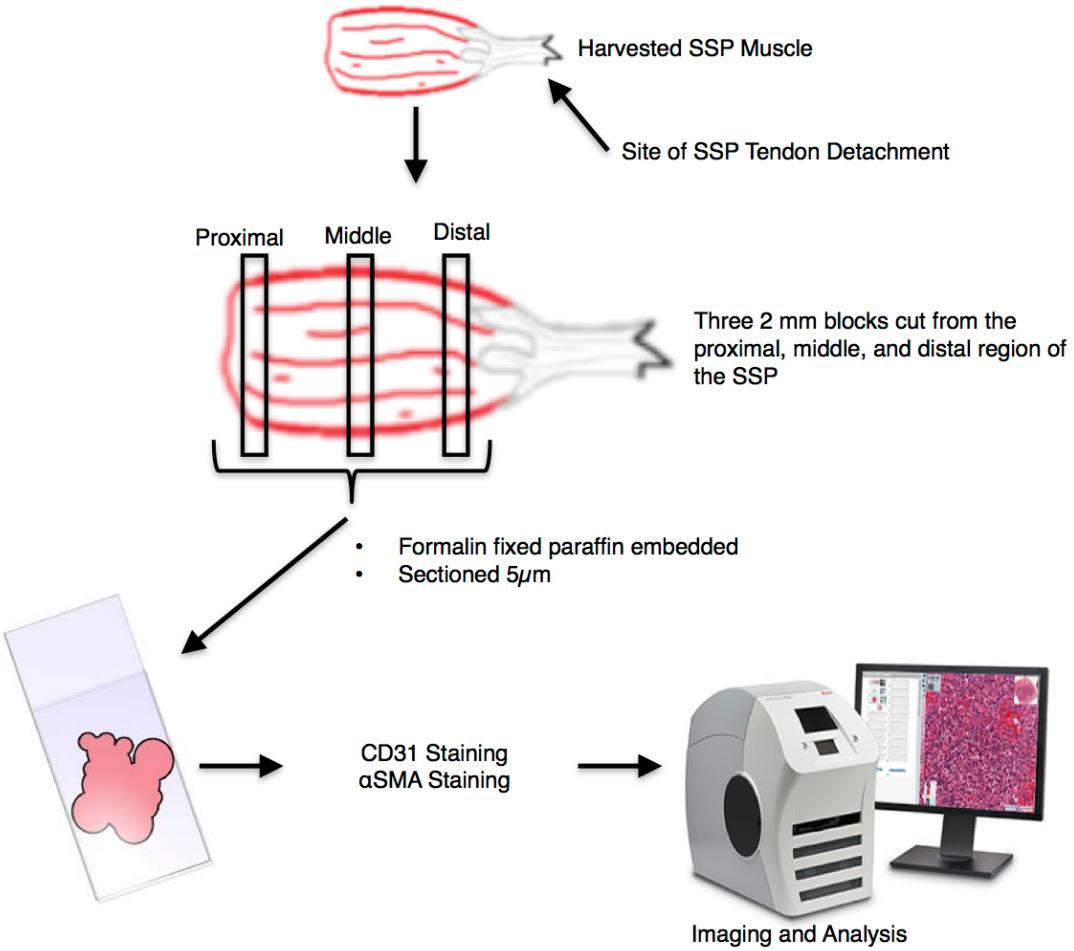

Figure 2.2. Experimental procedure for preparation of histology samples. Flow diagram for preparation, staining, and analysis of SSP muscles following harvest. SSP muscles from all three experimental groups undergo the same processing, staining, and analysis protocol as outlined above. Three 2-mm sections are taken from the distal, middle, and proximal regions of the SSP muscle, formalin fixed and paraffin embedded. The embedded paraffin blocks were then sectioned at 5μm thickness for either CD31 or αSMA immunohistochemistry. All samples were then imaged and analyzed.

2.6 Immunohistochemistry

CD31

A commercially available, pre-diluted cluster of differentiation 31 (CD31) antibody (131M-98, Cell Marque, Rocklin, CA, USA) was used to selectively stain the CD31 epitope expressed in the endothelial layer of vascular structures. The protocol provided by the manufacturer was modified to optimize staining. Tissue sections were deparaffinised in toluene and graded alcohols and underwent a heat and pressure induced epitope retrieval in a sodium citrate buffer (pH 9) at 110ºC for 13 minutes using an AR Histo S5 Rapid Microwave Histoprocessor (PALM Histology Core Facility, University of Ottawa). The sections were incubated with Peroxidazed 1 (Biocare Medical, Pacheco, CA, USA) to remove endogenous peroxidases 10 minutes. The sections were then blocked with Background Sniper (Biocare Medical, Pacheco, CA, USA) for 20 minutes. Tissues were incubated with the primary CD31 antibody for one hour at room temperature. After decanting the primary antibody, the sections were incubated with the secondary goat-anti-mouse IgG antibody (ab6789, Abcam, Cambridge, UK) for 1 hour at room temperature. The sections were developed using 3, 3'-diaminobenzidine (Biocare Medical, Pacheco, CA, USA) for 1 to 3 minutes. The sections were then incubated with Mayer's hematoxylin for 1 minute. Excess hematoxylin was removed in running water followed by 10 dips in acid alcohol, a rinse in water, and incubation in ammonia water for one minute. Sections were dehydrated by four dips in: 50%, 70%, 100%, and 100% ethanol followed by 4 dips in toluene three times. Slides were then mounted and preserved using Permount® (Thermo Fisher Scientific, Waltham, MA, USA). All staining was done using appropriate controls which included: positive control with human tonsil, negative control with human tonsil, and negative

control with SSP muscle. Negative controls correspond to incubation with Tris-buffered saline as a replacement for primary antibody incubation.

For analysis, all sections were scanned using an Aperio CS2 ScanScope (Leica Biosystems, Vista, CA, USA) and whole SSP muscle cross-sections were digitized. From each SSP muscle cross-section, seven fields of view (FOV) were randomly placed throughout the SSP muscle cross-section at 1X magnification as shown in Figure 2.3. FOVs each measured 0.855mm x 0.530mm ($0.453mm^2$). Stained vascular structures within each FOV were manually counted. Vascular structures were identified using the following criteria: positive CD31 staining, one or more stained endothelial nuclei, and located within the intramuscular space. Thick vascular structures were distinguished from the total number of vascular structures and according to the following criteria: positive CD31 staining, vascular wall thickness greater than 15µm, and a diameter greater than 50µm.

αSMA

Alpha smooth muscle actin (αSMA) was chosen to stain the smooth muscle cells present in vascular structures and to evaluate the thickness of vascular structures. Tissue sections were deparaffinised in toluene and graded alcohols and no epitope retrieval was required to obtain positive staining. The sections were incubated with Peroxidazed 1 (Biocare Medical, Pacheco, CA, USA) for 10 minutes to remove endogenous peroxidases and then incubated with Background Sniper (Biocare Medical, Pacheco, CA, USA) for 20 minutes to reduce background staining. The sections were then incubated with an anti-αSMA antibody (ab8717, Abcam, Cambridge, UK) for 1 hour at room temperature. After incubation with the primary antibody, a secondary goat-anti-mouse IgG antibody (ab205719, Abcam, Cambridge, UK) was incubated with the tissue for 1 hour at room temperature. The sections were developed using 3, 3'-

diaminobenzidine (Biocare Medical, Pacheco, CA, USA) for 1-3 minutes. The sections were then incubated with Mayer's hematoxylin for 1 minute. Excess hematoxylin was removed in running water followed by 10 dips in acid alcohol, a rinse in water, and incubation in ammonia water for one minute. Sections were then dehydrated by four dips in: 50%, 70%, 100%, and 100% ethanol followed by 4 dips in toluene three times. Slides were then mounted and preserved using Permount® (Thermo Fisher Scientific, Waltham, MA, USA). All staining was done using controls which included: positive control with human liver, negative control with human liver, and negative control with SSP muscle. Negative controls correspond to incubation with Tris-buffered saline as a replacement for primary antibody incubation.

To analyze αSMA in each SSP muscle cross-section from the detachment and delayed reattachment group, a light microscope (Olympus BH-2, Tokyo) was used to visualize staining at 33X magnification. Five FOVs were selected in each SSP muscle cross-section if they had positive αSMA staining in a minimum of one vascular structure. The FOVs each measured 0.628mm x 0.471mm (0.296mm^2) were captured using a Marlin G080C digital camera (Allied Vision Technologies) with AVT Smartview 1.5.1 software. Vascular structures were identified using the following criteria: positive αSMA staining, one or more stained endothelial nuclei, and located within the intramuscular space. The thickness of each vascular structure in each FOV was measured three locations and averaged using ImageJ Software (Version 1.51, US National Institute of Health, Bethesda, MD, USA). Data is presented as average thickness of αSMA staining (μm) ± one standard deviation.

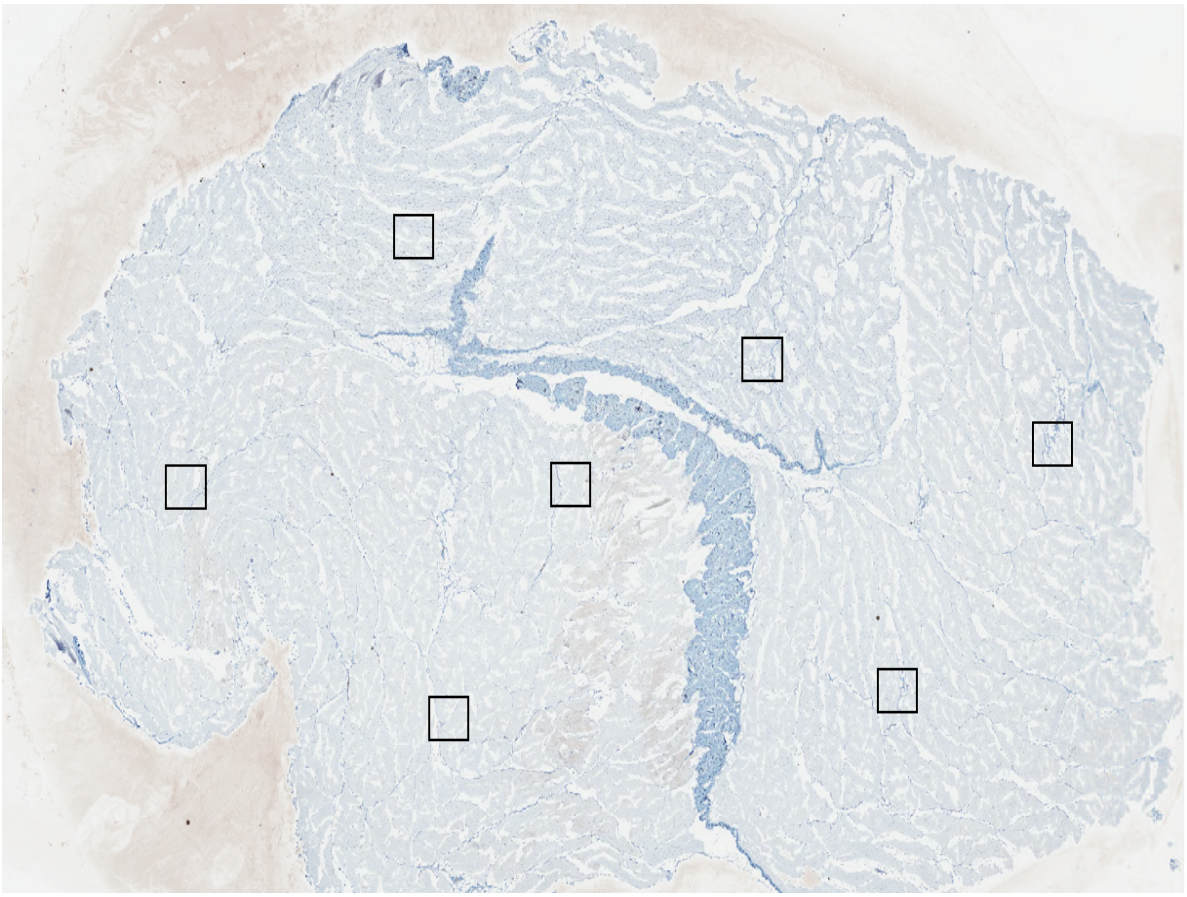

Figure 2.3. Representative distribution of 7 FOV used for CD31 immunohistochemistry analysis. SSP muscle section has been stained with CD31 and counterstained with Mayer's hematoxylin. Whole SSP muscle section is at 1X magnification when 7 FOV are randomly placed throughout the SSP muscle. CD31 staining is not visible at 1X magnification. Vascular structures within each FOV were manually counted following outlined criteria.

2.7 Intramuscular Fat Staining and Analysis

Intramuscular fat data from the same muscle specimens has been previously published by Trudel et al., and was available for the detachment, and delayed reattachment groups[26,51]. Intramuscular fat was quantified using to the following protocol. In brief, 1-mm cross-sections were cut from the distal, middle, and proximal regions of the SSP muscle and fixed in 10% neutral buffered formalin. Following formalin fixation, SSP muscle cross-sections were incubated in 5% potassium dichromate and 2% osmium tetroxide for two weeks, fixing intramuscular fat black. The SSP muscle cross-sections were then embedded in paraffin and cut in 6μm thick sections, mounted and imaged at 6.7X magnification. Using ImageJ software (US National Institute of Health, Bethesda, MD, USA) the intramuscular fat content was measured in each SSP muscle cross-section as a percentage of total area. Data from the analysis of intramuscular fat staining was provided for this study for the detachment and delayed reattachment groups[26,51].

2.8 Statistical Analysis

The number of vascular structures from 7 FOVs per muscle section are reported as median ± standard deviation. The percentage of thick vascular structures was expressed as (the number of thick vascular structures / total number of vascular structures) x 100 (%). To determine if there was a significant change in vascularization between different locations, time, and conditions, one-way ANOVA and unpaired t-tests were used. For detachment only group, all data from the operated samples was pooled over different time points and the locations and similarly for the control group to determine if there was a statistically significant difference using one-way ANOVA. If statistical significance was reached, p less than 0.05, the data was further subset into individual groups for time, location, and experimental group and unpaired t-tests

were used to determine if there was a statistically significant difference at any time point or location. The immediate and delayed reattachment groups were analyzed using the same strategy; initial step of pooling all data and application of one-way ANOVA and if significance measured, then identifying group differences using unpaired t-test. The same protocol for statistical analysis of data was used to determine if there was a statistically significant change in the percentage of thick vascular structures in the delayed reattachment group. A p-value of less than 0.05 indicated statistical significance and all data was analyzed with R Software (Version 1.0.153).

Pearson correlations were used to determine if a significant correlation existed between the number of vascular structures and intramuscular fat accumulation. Previously published intramuscular fat data was matched with vascularization data from the same muscle and if either portion of data was missing from a specimen, the specimen was excluded from the analysis. First, the data was analyzed by pooling experimental groups over time and location and similarly for corresponding controls. The relationship between intramuscular fat accumulation and vascularization was evaluated through Pearson correlations. If the pooled group reached statistical significance, the group was further divided into locations while pooling over time points. A p-value of less than 0.05 indicated statistical significance and all data was analyzed using R Software (Version 1.0.153).

To analyze the thickness of vascular structures in the detachment and delayed reattachment group the 5 FOVs per muscle section were reported as average thickness ± standard deviation. Vascular thickness is not consistent between locations in the skeletal muscles therefore muscle locations were not compared. A one-way ANOVA was used to determine if statistically significant differences in vascular thickness were present between experimental groups and times

within a given location. If statistical significance was reached unpaired t-tests were used to determine the location of significance. Statistical significance was reached when the p-value was less than 0.05.

3.0 Results

3.1 Vascular Density

The first step to quantify SSP muscle vascular density was to optimize the CD31 immunohistochemistry protocol. This was done by altering three main steps of the immunohistochemistry protocol; antigen retrieval, primary antibody incubation, and secondary antibody incubation. Modifications included changing the pH, concentration, duration, temperature, and pressure at which each step is carried out. The protocol yielding the most specific and intense staining included an antigen retrieval step at pH 9 in a sodium citrate buffer at 110ºC for 13 minutes in a pressurized environment. This was followed by incubation with a clinical pre-diluted CD31 antibody (131M-98, Cell Marque, Rocklin, CA, USA) for 1 hour at room temperature. Tissue sections were then incubated with the secondary goat anti-mouse IgG (ab6789, Abcam, Cambridge, UK) for 1 hour at room temperature. Specificity of this staining was demonstrated by omitting incubation with the primary antibody in SSP muscle sections as well as for human tonsil sections as shown in Figure 3.1.

Histology sections from SSP detachment, immediate reattachment, and delayed reattachment groups were examined to assess changes in number of CD31 stained vascular structures of the SSP muscle. Brown CD31 stained vascular structures were visible in SSP muscle sections of all three experimental groups (Figures 3.2, 3.4, and 3.6, Panels A to F). Each panel represents a FOV used to count the blood vessels. In the detachment group the distal portion of the SSP muscle had an elevated vascular density that reached statistical significance 12 weeks after detachment (4.78±2.49 vs 2.44±0.088 vascular structures; $p=0.024$) when compared to control SSP muscles (Figure 3.3). Representative histology images for the immediate reattachment groups are presented in Figure 3.4 and quantitative analysis is presented

in Figure 3.5. The median number of vascular structures observed in the immediate reattachment group was consistent over time ($p=0.601$), location ($p=0.560$), and with control specimens ($p=0.0620$). Images of SSP muscle sections from the delayed reattachment groups and controls are presented in Figure 3.6 and the quantitative analysis in Figure 3.7. The number of blood vessels in the delayed reattachment group was similar in the regions of the SSP muscle ($p=0.385$), over time ($p=0.783$), and not statistically significant from control specimens ($p=0.696$, Figure 3.7).

Blood vessels with thick vascular walls appeared in some sections, primarily in the detachment and delayed reattachment group. Thick vascular structures were characterized by: positive CD31 staining, vascular wall thickness greater than 15μm, and a diameter greater than 50μm. Blood vessels with thick vascular walls were observed in the delayed reattachment group (Figure 3.6, Panels A, B C, and D). An increase in thick vascular structures was not observed in the detachment only or the immediate reattachment groups. There was a higher mean percentage of thick vascular structures in SSP muscles after delayed tendon reattachment in seven of the nine time-points and locations when compared to controls but not statistically significant in most groups (Figure 3.7, and Table 3.1). Statistical significance was reached in the 4+12 week group in the distal region of the SSP muscle compared to controls ($p=0.025$, Table 3.1).

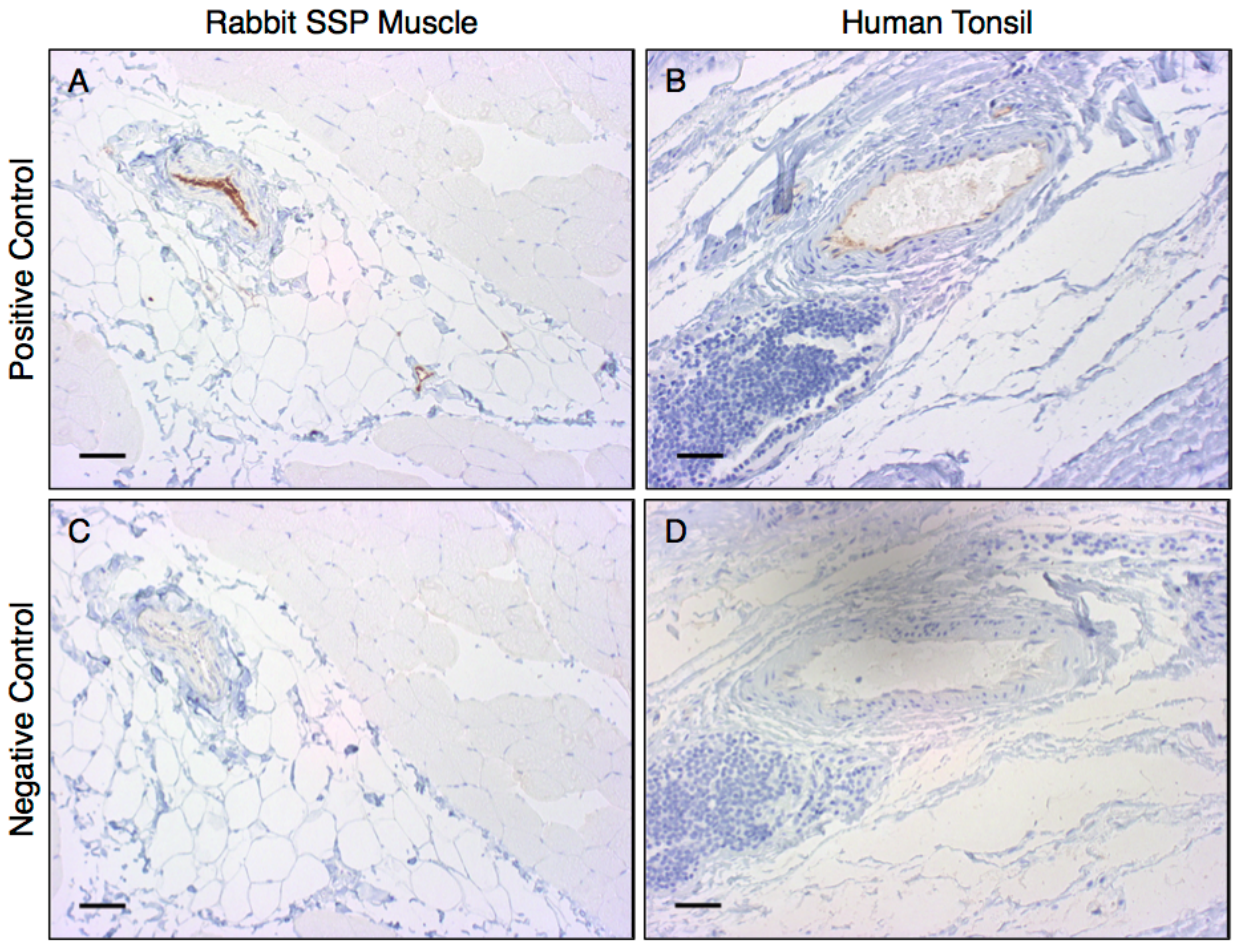

Figure 3.1. CD31 immunhistochemical staining of vascularization in the SSP muscle and human tonsil. Verification of CD31 immunohistochemistry using SSP muscle cross-sections (A, C) and human tonsil (B, D). Negative controls were not incubated with the primary antibody to verify specificity of the CD31 staining. Positive CD31 staining is brown. Human tonsil was used as a positive control because antibody had been verified in this tissue. All samples were counterstained with hematoxylin staining nuclei blue. Original magnification is 33X and scale bars indicate 50µm.

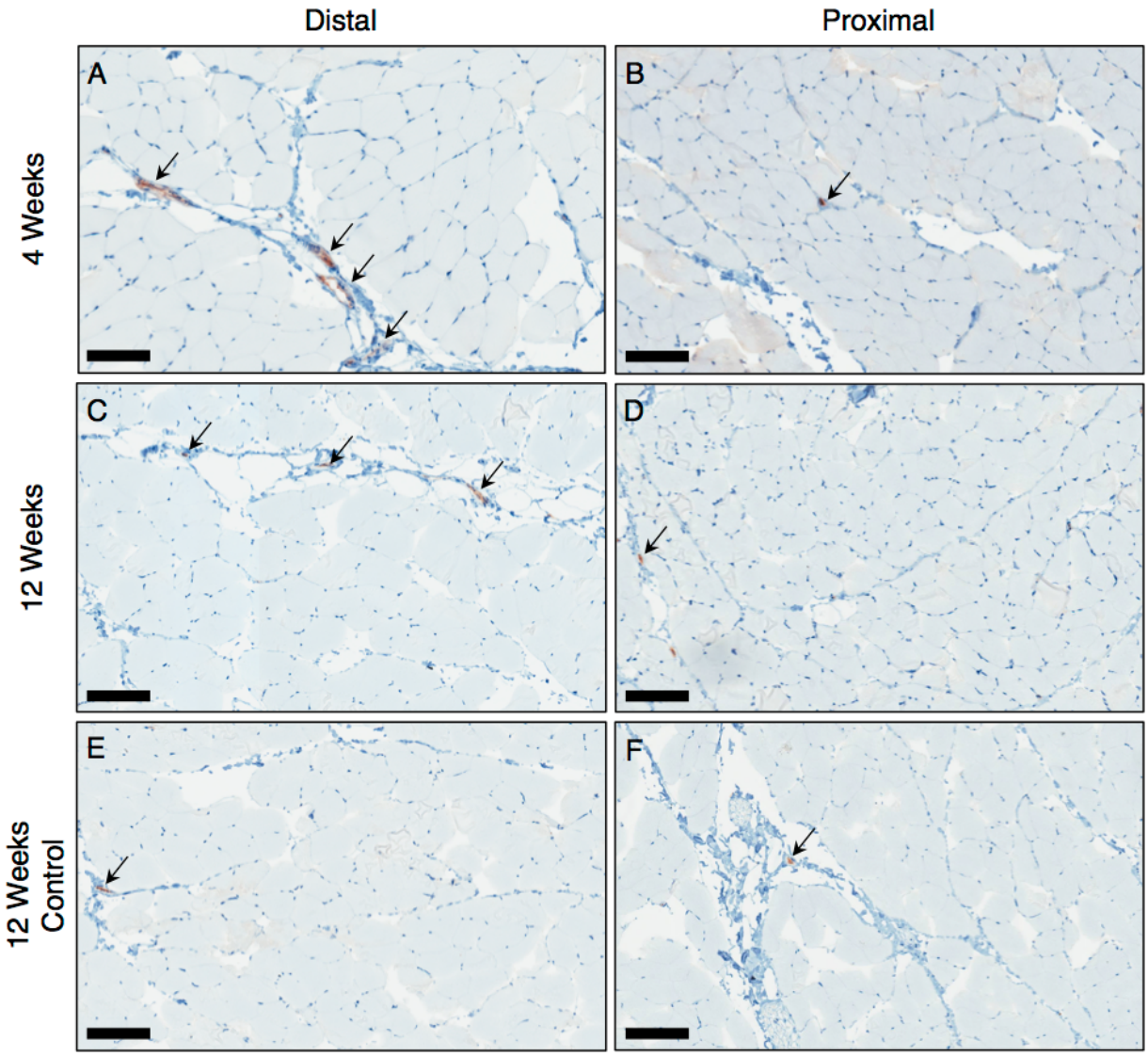

Figure 3.2. FOVs of SSP muscle after SSP tendon detachment. Panels A-F: micrographs of entire FOV from sagittal sections of the SSP muscle at distal and proximal regions 4 and 12 weeks after SSP tendon detachment. Vascular structures (black arrows) were stained with a CD31 antibody (brown) and counterstained with hematoxylin (blue). Distal SSP muscle sections (A, C) showed more vascular structures at 4 weeks after detachment compared to proximal sections (B, D) of the same SSP muscle and compared to sections from the control groups (E, F) but was not statistically significant. Original magnification is 20X and scale bars indicate 100μm.

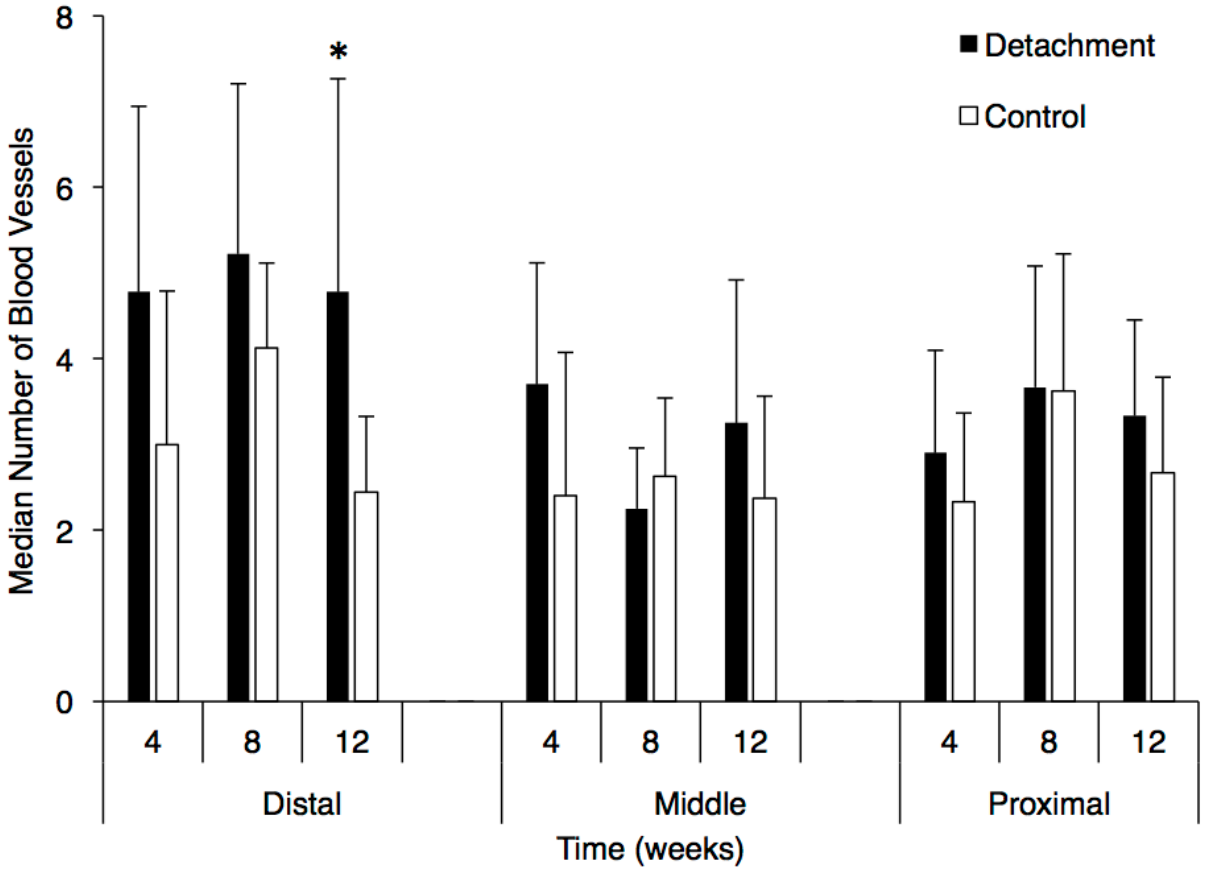

Figure 3.3. Median number of vascular structures in the detachment group. The median number of vascular structures of 7 FOVs was averaged for every group and the graph shows the median number of vascular structures ± one standard deviation. More vascular structures were found in the distal SSP muscle 12 weeks after SSP tendon detachment when compared to age-matched controls ($p=0.024$). Statistical significance is when p is less than 0.05 and is indicated by '*'.

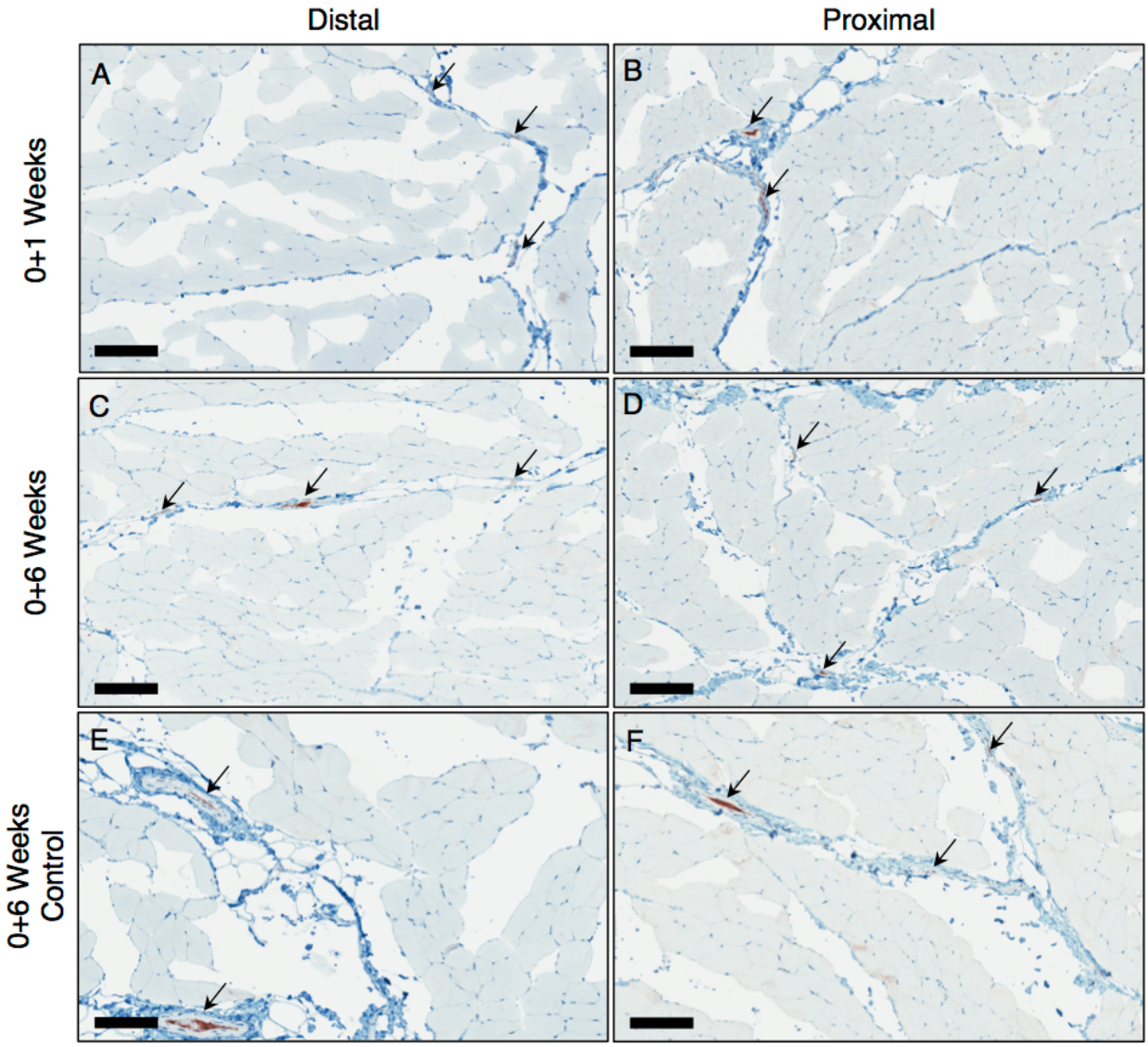

Figure 3.4. FOVs of SSP muscles after detachment and immediate reattachment. Micrographs of entire FOV of sagittal sections of distal and proximal regions of the SSP muscle reattachment group at 0+1 (A, B) and 0+6 weeks (C, D) and age-matched controls (E, F). Vascular structures stained with a CD31 antibody (brown and indicated with arrows) and myocytes stained with hematoxylin (blue). Original magnification is 20X and scale bars indicate 100µm.

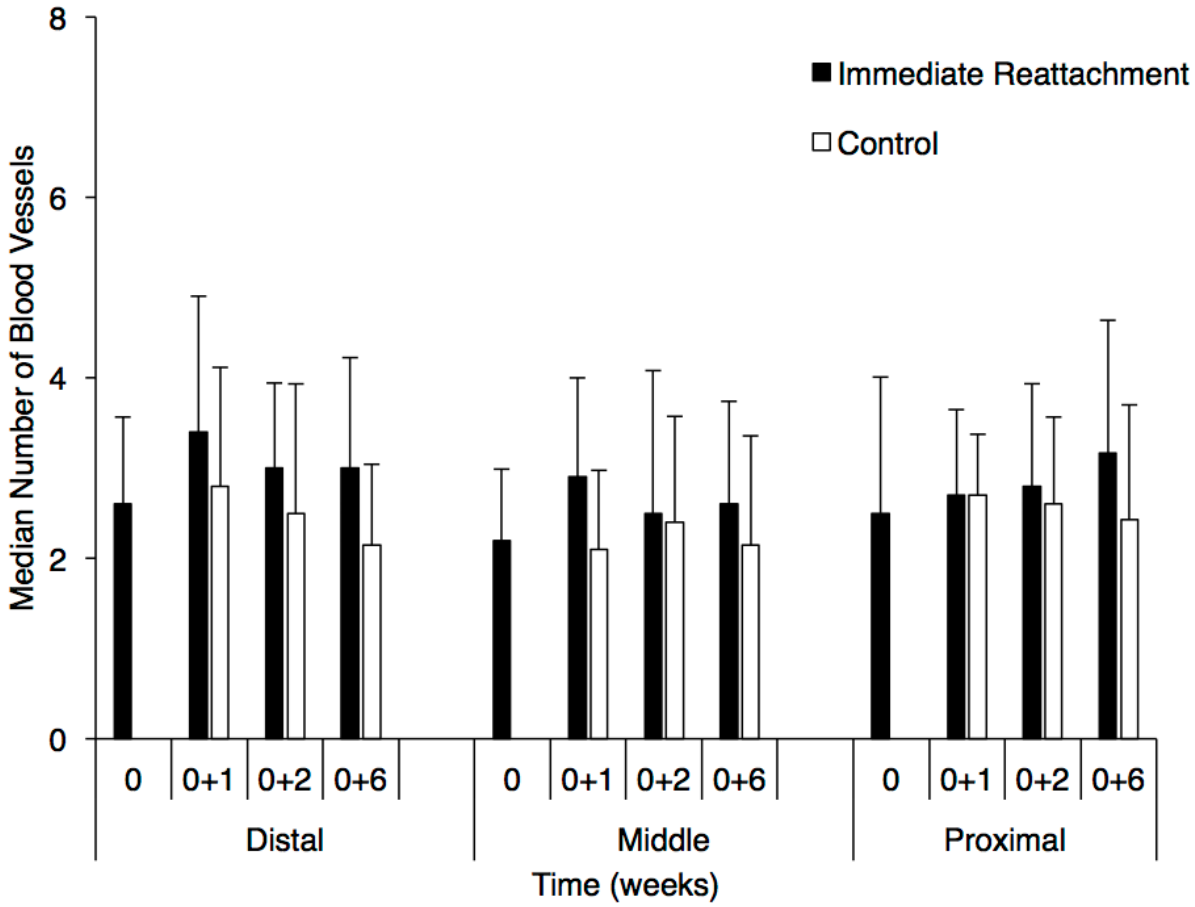

Figure 3.5. Median number of vascular structures found in the detachment and immediate reattachment group. The median number of vascular structures of 7 FOVs was averaged for every group and the graph shows the median number of vascular structures ± one standard deviation. There was no statistically significant difference between experimental and controls groups at any time point or location.

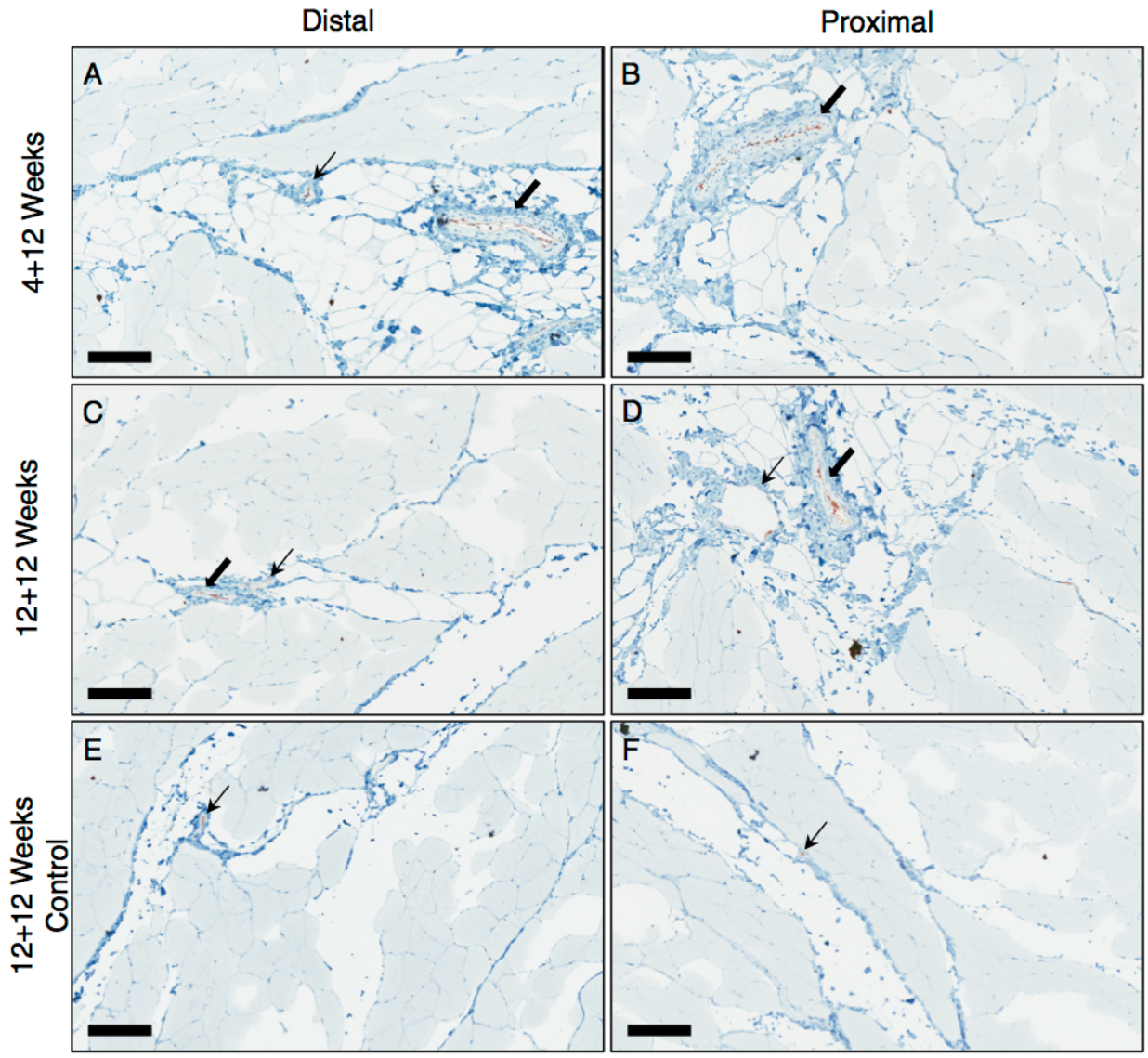

Figure 3.6. FOVs of SSP muscles 12 weeks after surgical reattachment. Micrographs of entire FOV of sagittal sections of distal and proximal regions of the SSP muscle reattachment groups at 4+12 (A, B) and 12+12 weeks (C, D) and age-matched controls (E, F). Vascular structures stained with a CD31 antibody (brown and indicated with arrows) and myocytes stained with hematoxylin (blue). Some vascular structures with thick walls (indicated with thick arrows) were observed in the reattachment groups (A,B,C,D) but not in controls (E,F). Original magnification is 20X and scale bars indicate 100μm.

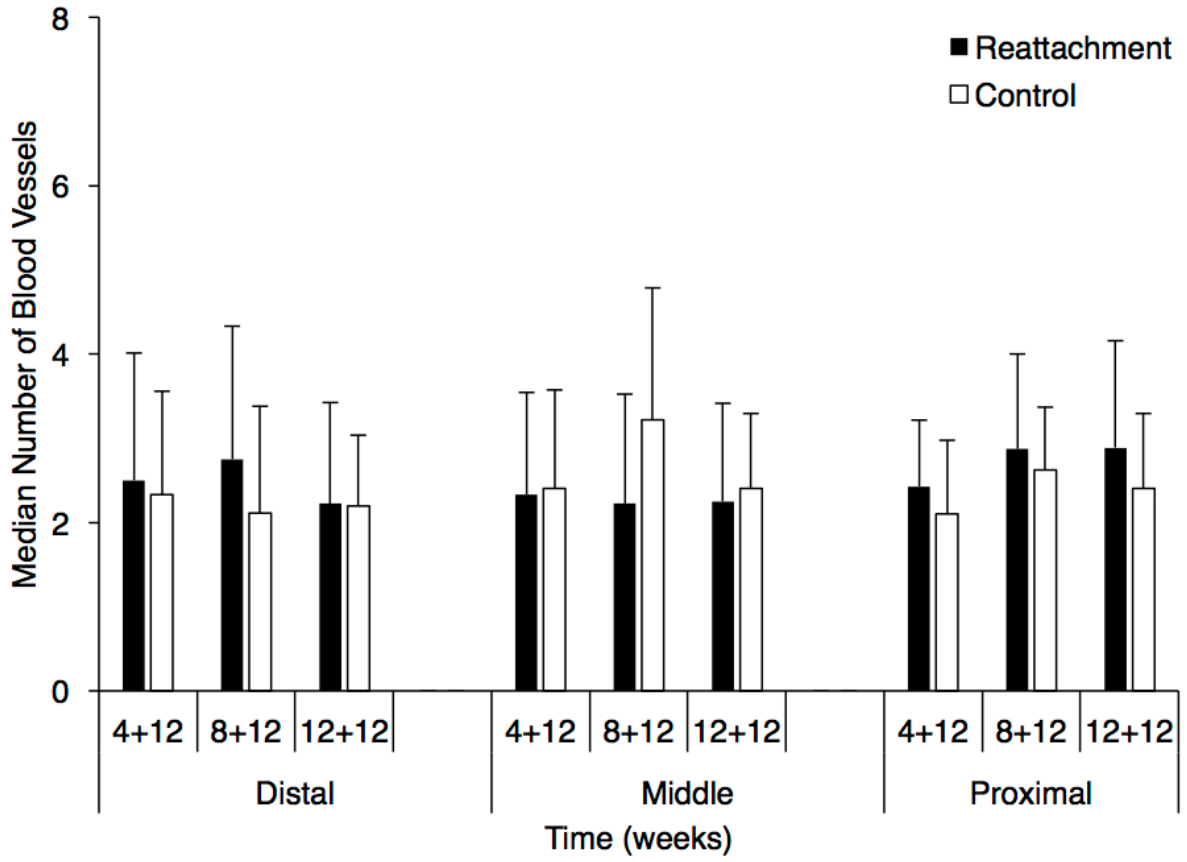

Figure 3.7. Median number of vascular structures found in the delayed reattachment group. The median number of vascular structures of 7 FOVs was averaged for every group and the graph shows the median number of vascular structures ± one standard deviation. There was no statistically significant difference in the number of blood vessels between experimental groups and locations.

	Distal			Middle			Proximal		
	4 Weeks	8 Weeks	12 Weeks	4 Weeks	8 Weeks	12 Weeks	4 Weeks	8 Weeks	12 Weeks
Detachment	0	0.300	1.509	0.286	0.658	1.157	1.080	2.794	3.298
Control	0	0.463	0	0	3.102	3.662	4.019	1.405	1.740
p-value	1.000	0.773	0.128	0.343	0.290	0.265	0.118	0.197	0.353
	Distal			Middle			Proximal		
	4+12 Weeks	8+12 Weeks	12+12 Weeks	4+12 Weeks	8+12 Weeks	12+12 Weeks	4+12 Weeks	8+12 Weeks	12+12 Weeks
Reattachment	6.001	3.248	7.172	6.700	7.393	9.199	4.382	5.109	3.343
Control	0.463	4.253	1.740	3.861	5.364	11.444	2.764	2.633	2.914
p-value	0.025*	0.604	0.249	0.347	0.724	0.721	0.446	0.299	0.806

Table 3.1. Percentage of vascular structures with thick vascular walls in the detachment and delayed reattachment SSP groups for all time points and muscle locations. Vascular structures were counted as thick when they met the following criteria: positive CD31 staining, greater than 15μm vascular wall thickness, and a diameter of 50μm or larger. The number of thick vascular structures / total number of vascular structures for each FOV are presented with p-values. Statistical significant is reached when p is less than 0.05 and is indicated by '*'.

3.2 Intramuscular Fat

The intramuscular fat content from the detachment only and detachment and delayed reattachment group from the same specimens was previously reported and representative micrographs of osmium tetroxide stained SSP cross-sections are presented in Figure 3.8[26,51]. The intramuscular fat stained in black was more prominent in the distal portion of the SSP muscle 12 weeks after detachment. Proximal and middle sections of the SSP muscle showed lower intramuscular fat compared to detached distal sections. The intramuscular fat accumulation was previously characterized in the same specimen corresponded to a gradient from high levels of intramuscular fat in the distal end where the SSP tendon was detached to low intramuscular fat content at the proximal end of the SSP muscle[26]. Similarly, increased fat was observed in the distal portion of the SSP muscles from the reattachment groups (Figure 3.8) and progressed over time[51]. The intramuscular fat data was not available for the immediate reattachment group.

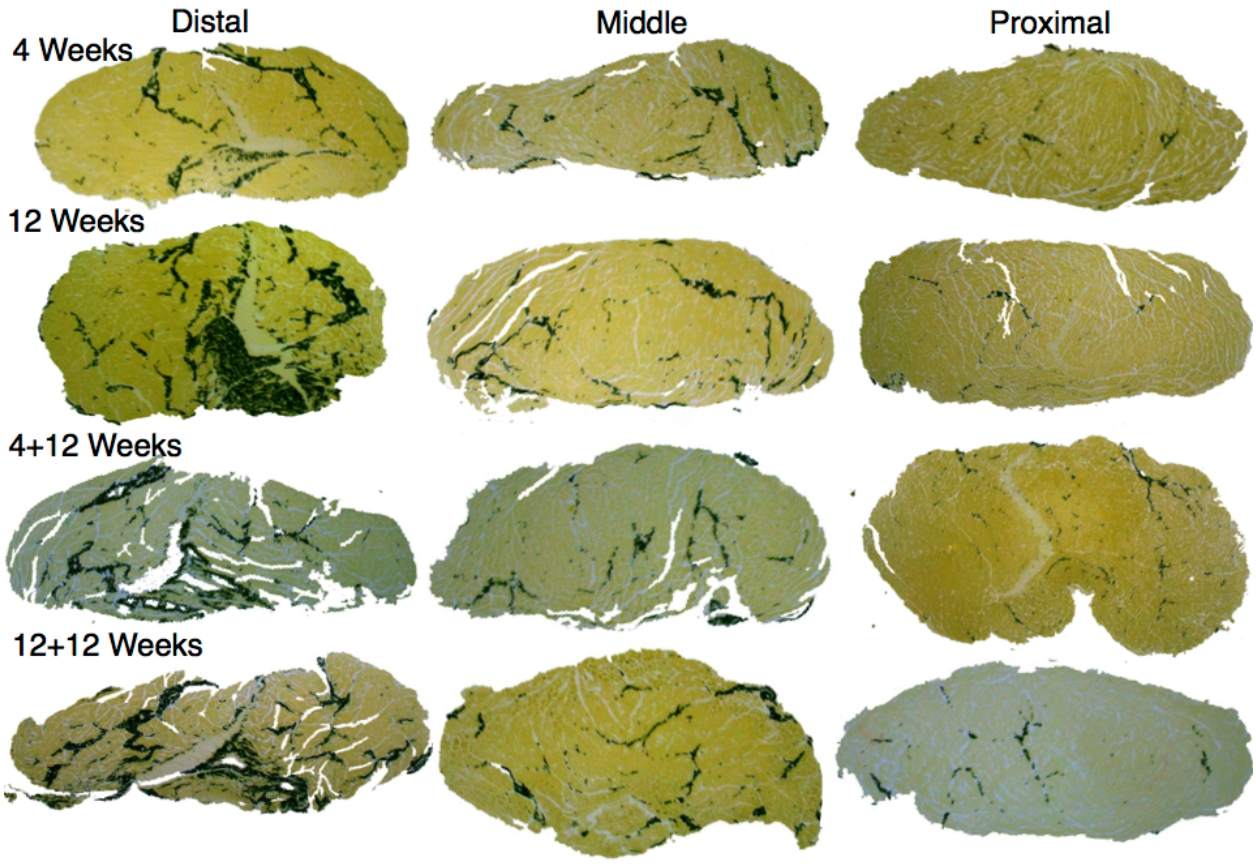

Figure 3.8. Micrographs of entire SSP muscle cross sections fixed with osmium tetroxide from the detachment only and detachment and delayed reattachment groups. Fat accumulation was more pronounced in the distal section of the SSP muscle after detachment and statistically significant at 12 weeks after detachment when compared to controls. After detachment, the progressive fat accumulation in the distal region of the SSP muscle was not reversed by surgical reattachment as shown in the 4+12 and 12+12 SSP muscle cross-sections. Unoperated control specimens showed low intramuscular fat that was comparable to intramuscular fat accumulation in the proximal region of the SSP muscle (data not shown). Original magnification is 6.7X.

3.3 Vascular Density and Intramuscular Fat Association

Linear models were fit to the data from the detachment and delayed reattachment groups to determine if correlations between the number of vascular structures and intramuscular fat were statistically significant. In the first analysis, samples were pooled over time and distal, middle, and proximal regions of the SSP muscle for each of the detachment and control groups. Blood vessel numbers and corresponding intramuscular fat content for the detachment only group was plotted and results from the linear model fit to data had a Pearson correlation coefficient of 0.2935 that was statistically significant ($p=0.0078$, Figure 3.9, Table 3.2). No statistically significant correlation was measured for the control group (-0.1986, $p=0.11$, Figure 3.9, Table 3.2).

In the second analysis, the data from the detachment group was divided into distal, middle, and proximal regions of the SSP muscle to determine if the association between intramuscular fat and vascularization was localized to a specific region and plots are presented in Figure 3.10. Results from the linear regression analysis of the number of vascular structures and corresponding intramuscular fat showed no significant correlation for detachment or control groups when divided into location (distal $p=0.092$, middle $p=0.058$, proximal $p=0.936$, Figure 3.10, Table 3.2).

An analysis of blood vessel number and intramuscular fat content was conducted for the delayed reattachment group and data was pooled over time and distal, middle and proximal regions and similarly for controls. Plotted data and linear regressions are presented in Figure 3.11. Neither control nor detachment groups showed a statistically significant correlation between number of vascular structures and intramuscular fat content ($p=0.645$, Table 3.2).

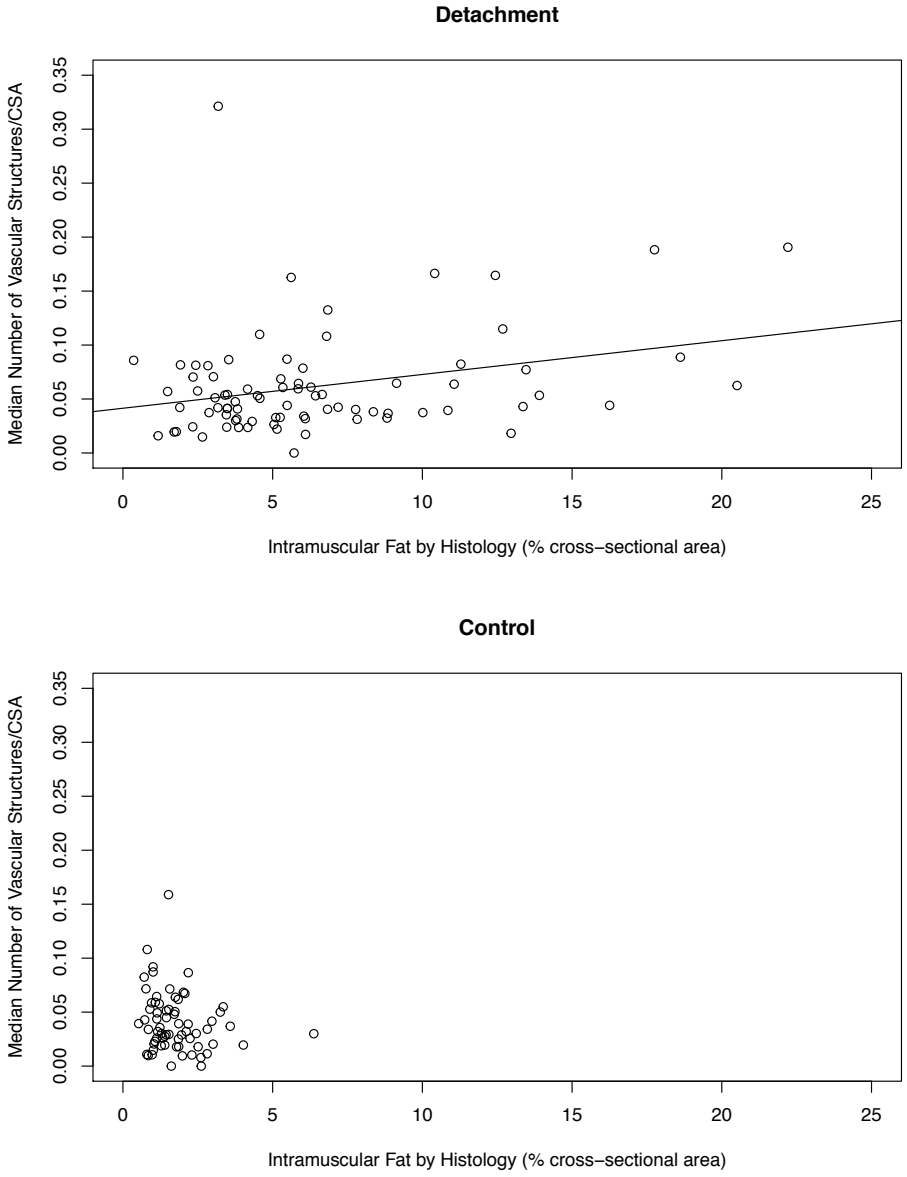

Figure 3.9. Correlation graphs of vascular structure medians and corresponding intramuscular fat accumulation following SSP tendon detachment. Detachment and control values were pooled over time (4, 8, 12 weeks) and SSP muscle location (distal, middle, proximal). The Pearson correlation coefficient was significant for the pooled detachment group (0.2935, p=0.0078). No significant correlation was found in the control group (-0.1986, p=0.1072). Exact p-values and Pearson correlation coefficients are reported in Table 3.2.

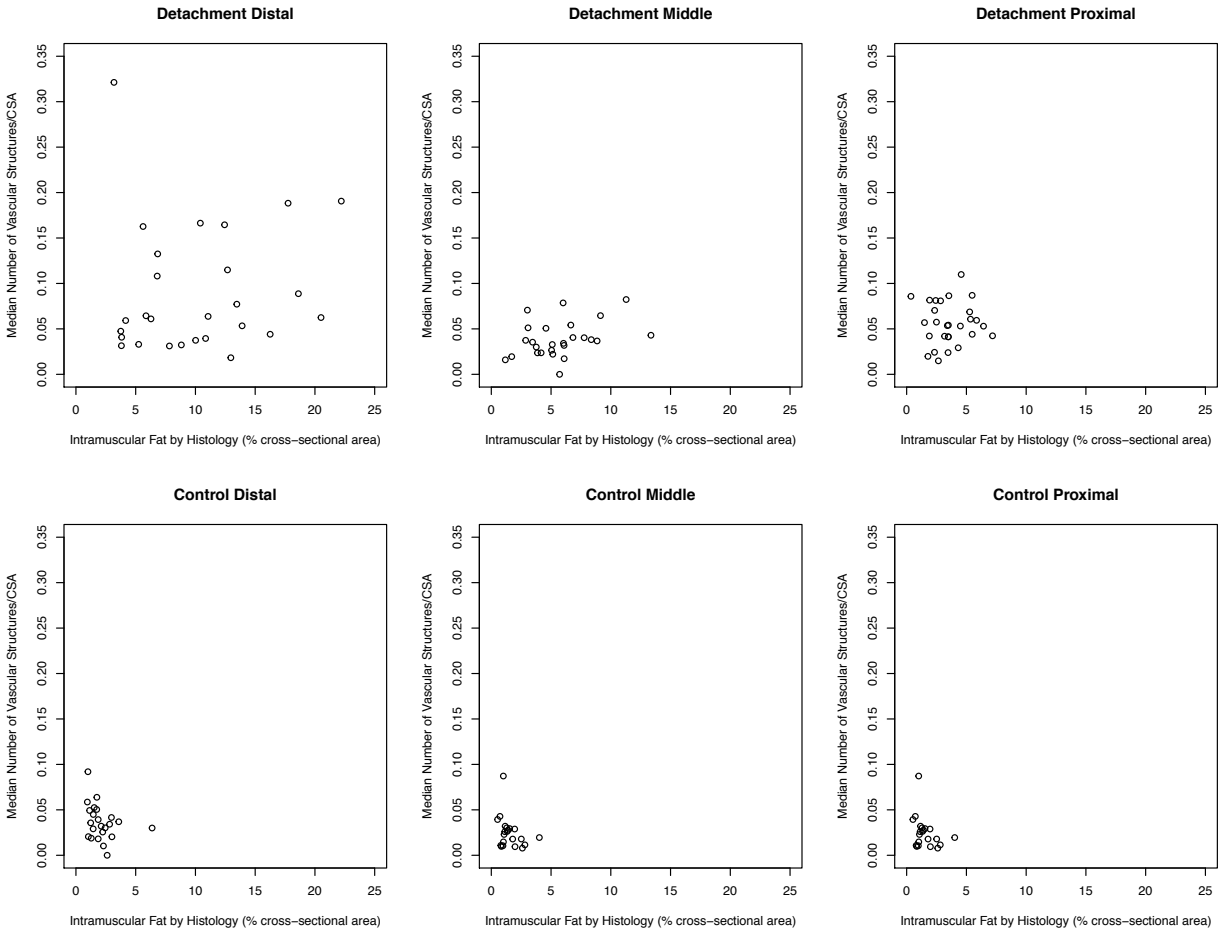

Figure 3.10. Correlation graphs of blood vessel number and intramuscular fat content for detachment groups; distal, middle, and proximal regions of the SSP muscle. A linear model was fit to each data set and Pearson correlation coefficients as well as p-values are reported in Table 3.2. No statistical significance was measured at any muscle location and all p-values were greater than 0.05.

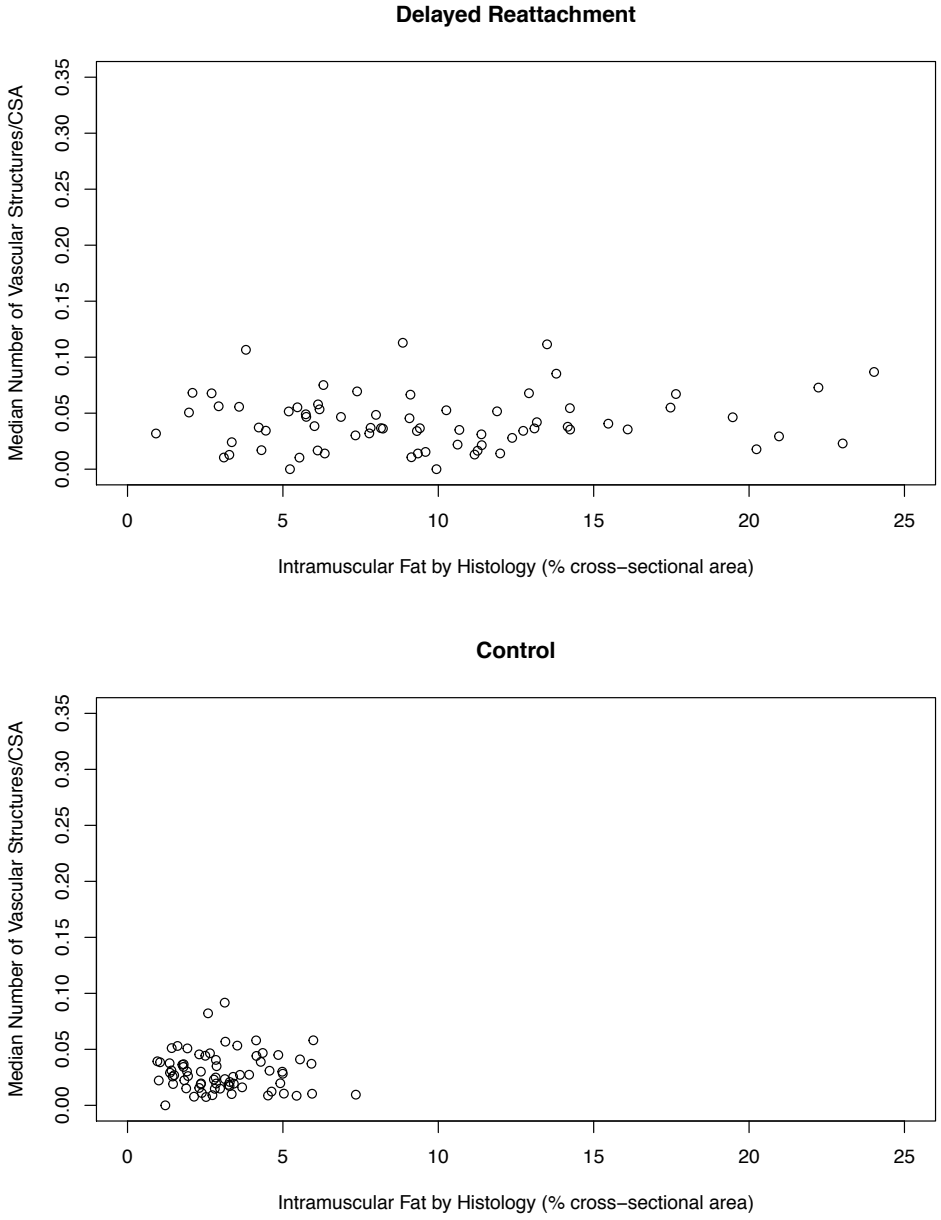

Figure 3.11. Correlation between vascularization and intramuscular fat after SSP tendon detachment and immediate reattachment and age-matched controls. Data from muscle regions (distal, middle, and proximal) and time points (4+12, 8+12 and 12+12 weeks) were pooled for each respective graph. There was no significant correlation between vascular density and intramuscular fat 12 weeks after SSP tendon reattachment. Exact p-values and Pearson correlation coefficients are reported in Table 3.2.

Comparison		Pearson Correlation Coefficient	p-value	n
Detachment Group	Control	-0.1986	0.107	67
	Experimental	0.2935	0.008*	84
	Experimental Distal	0.6496	0.092	27
	Experimental Middle	0.3762	0.058	26
	Experimental Proximal	0.0160	0.936	28
Reattachment Group	Control	-0.0527	0.665	70
	Experimental	0.0552	0.645	72

Table 3.2. Pearson correlation coefficients and exact p-values for all comparisons of vascular structure numbers and corresponding intramuscular fat content from all groups. Pearson correlation coefficients, exact p-values, and sample sizes for each group are indicated. Statistical significance was reached when p was less than 0.05 and is indicated by '*'.

3.4 Vascular Thickness

The observation of some blood vessels with increased vascular thickness in the delayed reattachment group prompted further investigation and the measurements of tunica media thickness. The smooth muscle layer of the blood vessels was stained with αSMA. To begin, the protocol for αSMA had to be optimized and specificity was demonstrated as shown in Figure 3.12. By varying the primary and secondary antibody concentrations and incubation times, staining was optimized and specificity confirmed. In the protocol used, antigen retrieval was not required to generate positive αSMA staining. Tissue sections were incubated with the primary anti-αSMA antibody (ab8717, Abcam, Cambridge, UK) at room temperature for 1 hour. The secondary goat-anti-mouse IgG antibody (ab205719, Abcam, Cambridge, UK) was added for 1 hour at room temperature. To verify specificity of staining, the primary antibody was omitted from the protocol when staining SSP muscle sections and using a control tissue of human liver, representative images are shown in Figure 3.12. Increased thickness of some blood vessel walls was observed in experimental SSP muscle sections when compared to unoperated controls (Figure 3.13, Panel A, B, C, and D). Statistical significance was reached in the distal region at 4+12 weeks ($p=0.012$) and 12+12 weeks ($p=0.012$) and in the proximal region at 4+12 weeks ($p=0.024$) when compared to age-matched controls (Figure 3.14, Table 3.3). There was no statistically significant difference in the thickness of vascularization in the middle region of the SSP muscle following delayed reattachment (4+12 weeks $p=0.344$, 8+12 weeks $p=0.160$, 12+12 weeks $p=0.607$). Average vascular thickness and exact p-values are shown in Table 3.3.

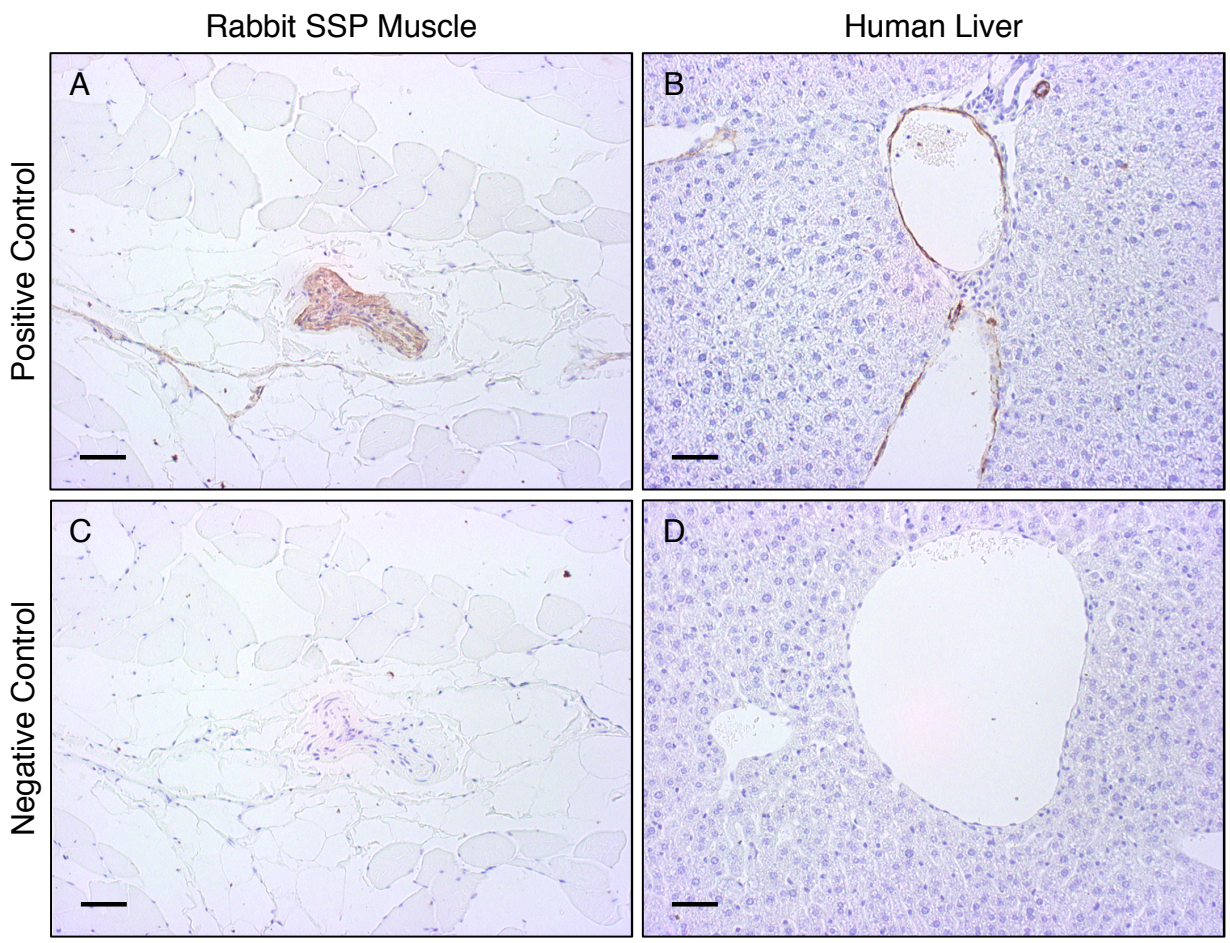

Figure 3.12. αSMA immunhistochemical staining of vascularization in the SSP muscle and human liver. Specificity of αSMA staining was demonstrated using SSP muscle cross-sections (A, C) and human liver tissue sections (B, D) by omitting the primary antibody incubation step in negative controls (C, D). Tissue sections from human liver were used as positive controls and αSMA was visible in brown. All samples were counterstained with hematoxylin staining nuclei blue. Original magnification is 33X and scale bars indicate 50μm.

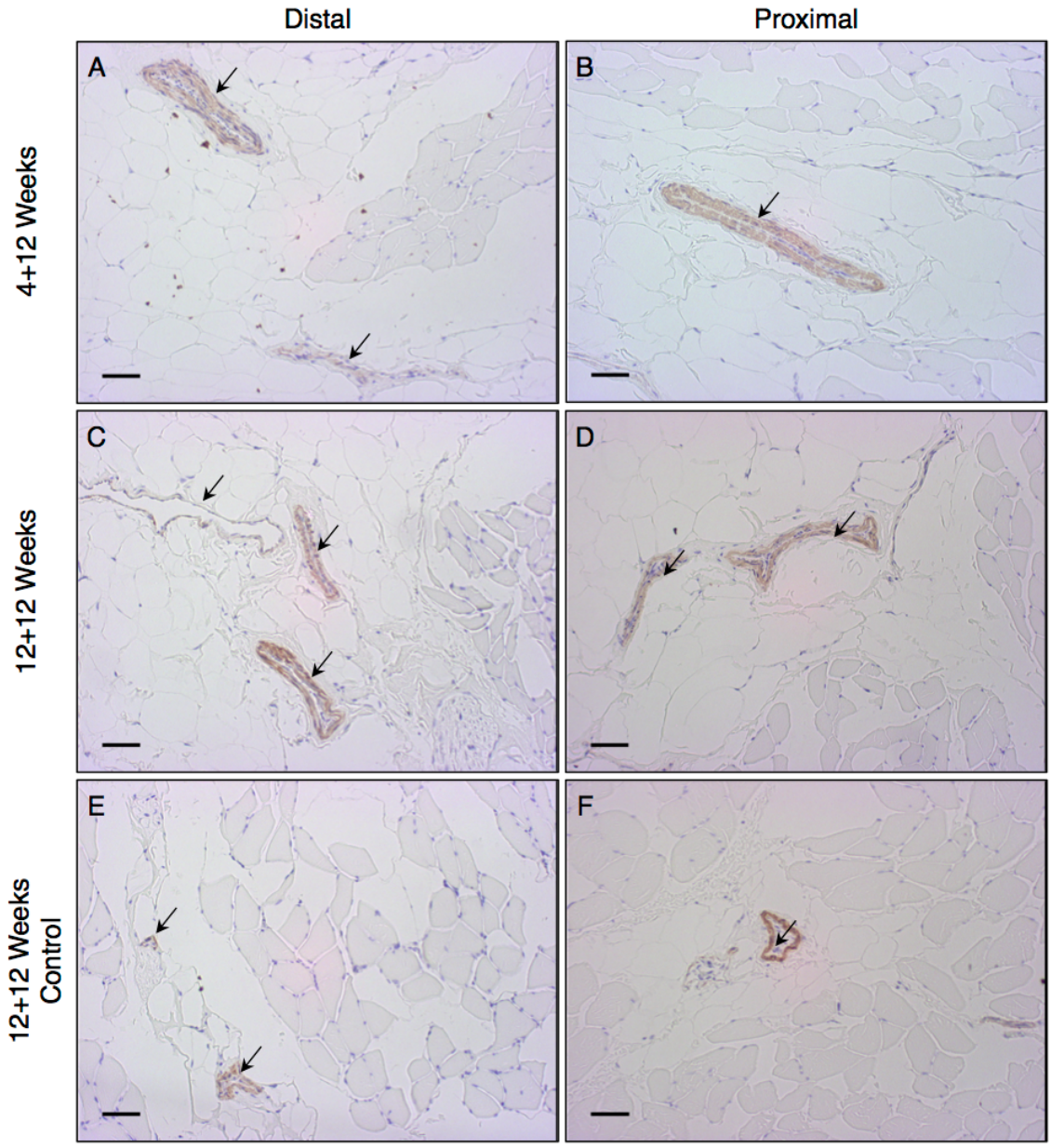

Figure 3.13. FOVs of αSMA staining in SSP muscles 12 weeks after surgical reattachment. Micrographs of entire FOV of sagittal sections of the distal and proximal regions of the SSP muscle reattachment group at 4+12 (A, B) and 12+12 weeks (C, D) and age-matched controls (E, F). Vascular structures stained with a αSMA antibody (brown and indicated with arrows) and nuclei stained with hematoxylin (blue). Original magnification is 33X and scale bars indicate 50μm.

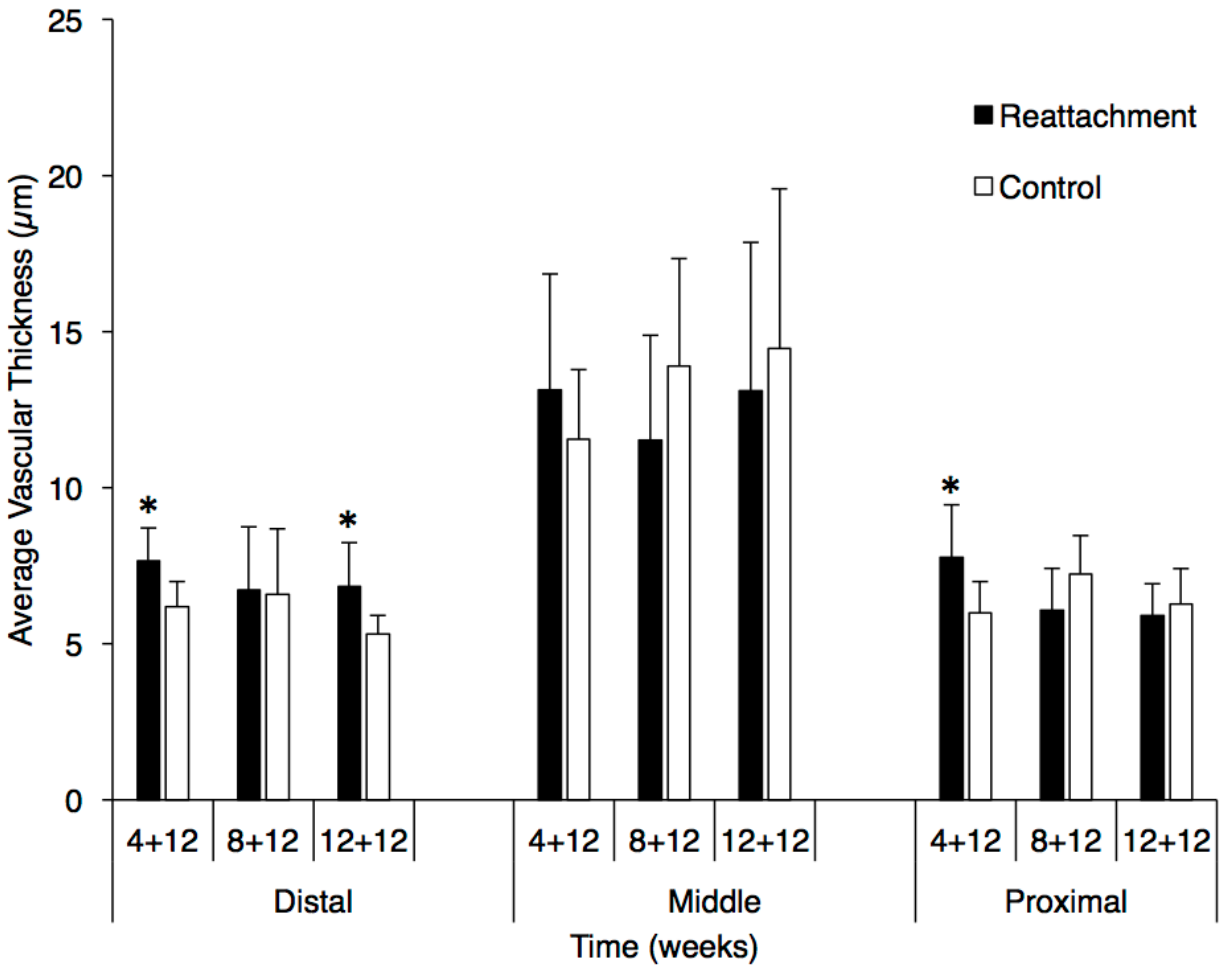

Figure 3.14. The average thickness of the vascularization in the delayed reattachment group. Graph shows average thickness of vascular walls for each group ± one standard deviation. The thickness of the same vessel was measured at 3 locations and averages are reported. Statistical significance was reached if the p-value was less than 0.05 is indicated by '*'.

	Distal			Middle			Proximal		
	4+12 Weeks	8+12 Weeks	12+12 Weeks	4+12 Weeks	8+12 Weeks	12+12 Weeks	4+12 Weeks	8+12 Weeks	12+12 Weeks
Delayed Reattachment	7.667	6.718	6.834	13.124	11.525	13.112	7.763	6.062	5.914
Control	6.182	6.591	5.304	11.553	13.890	14.473	5.980	7.244	6.264
p-value	0.012*	0.968	0.012*	0.344	0.160	0.607	0.024*	0.070	0.584

Table 3.3. Average thickness (μm) of vascular walls in the delayed reattachment groups. Thickness of a vascular structure was measured at three sites for each blood vessel and averaged between all vessels present in an FOV. The average thickness (μm) is presented for each time-point and location within the SSP muscle with age-matched controls and exact p-values. A p-value less than 0.05 is indicated by *.

4.0 Discussion

The purpose of this study was to characterize the vascularization of rotator cuff tears with and without surgical reattachment to contribute to the understanding of intramuscular fat accumulation. To achieve this, three experimental protocols of rotator cuff tear were studied; SSP tendon detachment, SSP tendon detachment and immediate reattachment, and SSP tendon detachment and delayed reattachment. Using CD31 immunohistochemistry, I examined the vascular density in tissue sections of the SSP muscle in three locations and at different times after detachment with or without reattachment. First, I will summarize my findings. A transient and localized increase in the number of blood vessels was observed only in the detachment group. The increase in vascular structures was localized in the distal portion of the SSP muscle near the site of tendon detachment. The increase in blood vessel number was not observed in the immediate or delayed reattachment groups. When quantifying the vascular density of the three experimental groups under the microscope, I observed blood vessels with thick vascular walls in specimens from the delayed reattachment group. The increased medial thickness of vessels was quantitated using immunohistochemistry and an antibody to detect αSMA of the medial layer of vascularization. There was a significant increase in medial thickness of the vascular structures in the delayed reattachment group in the distal and proximal regions. Lastly, the association between intramuscular fat and vascularization was significant in the detachment only group when data was pooled over time and location. No significant correlation was observed when data was subset into muscle locations after detachment or in the delayed reattachment group.

4.1 Vascular Density and Intramuscular Fat Accumulation

The first hypothesis was partially confirmed; vascular density was increased in the distal portion of the SSP muscle reaching statistical significance only at 12 weeks of tendon

detachment. At earlier time points, 4 and 8 weeks, there was an increase in vascular density when experimental specimens were compared to the control specimens but did not reach statistical significance. Intramuscular fat accumulation measured in the same specimens was significantly different when compared to control groups as early as 4 weeks following SSP tendon detachment and continued increasing through 12 weeks of detachment[26]. The significant increases in intramuscular fat and vascularization co-localized in the distal end of the muscle after 12 weeks of detachment only and not earlier after detachment[26]. The increase in intramuscular fat preceded the increase in vascular density in the experimental model of SSP tendon detachment without reattachment[26]. Overall, the locations of intramuscular fat and vascularization increases co-localized in the distal end of the SSP muscle but occurred at different times after tendon detachment.

When the SSP tendon was immediately repaired following detachment, no significant increase in vascular density was measured at any time point or location. Using the same specimens, a previous study reported an increase in intramuscular fat accumulation in the middle region of the muscle 1 week following immediate reattachment[72]. Two weeks following immediate reattachment of the SSP tendon the distal portion of the SSP muscle had a significant increase in intramuscular fat and 6 weeks after reattachment, the whole SSP muscle had a significantly increased intramuscular fat content when compared to controls[72]. Overall, previous results from the immediate reattachment studies indicate that intramuscular fat persisted in the absence of muscle retraction; achieved by immediately reattaching the tendon after sectioning[72]. I measured no significant increase in the number of vascular structures in the reattached muscles while intramuscular fat accumulation was previously documented in the same SSP muscles.

Therefore, my first hypothesis was not supported with regards to the immediate reattachment of the SSP muscle.

In the delayed reattachment group, there was no statistically significant increase in vascularization measured at any time point or location. The previously published data on intramuscular fat accumulation after delayed reattachment reported a significant increase in intramuscular fat measured after a 12-week healing period[51]. From the previous experiment in the distal regions, all time points 4+12, 8+12, and 12+12 weeks showed a statistically significant increase in intramuscular fat when compared to controls[51]. In the middle and proximal regions of the SSP muscle, only later time points, 8+12 and 12+12 weeks, showed an increase in intramuscular fat when compared to controls[51]. The first hypothesis was not verified with regards to the delayed reattachment group as vascularization did not significantly increase while intramuscular fat increased at all time points.

Our data is indicative of the dynamic nature of muscle vascularization in response to SSP tendon detachment with or without reattachment. Increased vascular density was limited to the distal portion of the muscle near the tendon detachment site at 4 weeks. There is a possibility that vascular changes could have occurred earlier than 4 weeks and would have preceded the intramuscular fat increase. Additional experiments including harvesting SSP muscle sections earlier than 4 weeks after detachment must be performed to test this possibility. The experimental protocol used to detach the SSP tendon; the sectioning of the distal SSP tendon, induced a response aimed at repairing the injury. The immediate response to injury was not studied in the project and for this reason, the earliest time point was set at 4 weeks after detachment.

The development of new blood vessels, angiogenesis, is a dynamic process that is highly regulated after tissue injury[54,73]. The tissue response includes early changes in blood flow, permeability and vascularization[54,87,88]. Initially, blood vessels near the injured area will dilate to allow for the delivery of blood factors to the site of injury, initiating the healing process and can persist for up to one week[89]. Blood vessels will also become more permeable to distribute nutrients and blood components at a faster rate[54,90]. Later after the injury, angiogenesis will occur and small vessels will develop to assist the repair process[54,90]. Vascular flow, permeability, and growth are controlled by soluble growth factors, membrane-bound proteins, and cell-to-cell interactions acting in concert to promote the elimination of damaged tissue and regenerate healthy tissues[73]. The fast changes in vascular properties are mediated by compounds such as histamines that promote vascular differentiation, remodeling, and overall increase in vascularization of the affected area[54]. In humans, remodelling of vascularization begins approximately 4 to 5 days after injury and continues until 23 days after injury in skeletal muscle[90]. Using a highly-regulated system to control vascularization allows the body to respond to injury including tendon tear[54,73,88,89,91]. An increase in the vascular density of the SSP tendon has been observed in ruptured SSP tendons samples harvested at the time of arthroscopic repair[80]. The mechanisms of tendon repair have been described in the Achilles tendon tear with emphasis on later events rather than immediate response to tear[89]. Some of the growth factors involved in angiogenesis are vascular endothelial growth factor (VEGF), fibroblast growth factor, and leptin[73,88]. These factors will promote the growth of vascularization but are also involved in controlling the inflammatory and immune response[89]. Of importance for the rotator cuff, VEGF was reported to be upregulated following a complete rotator cuff tear and was suggested to play an important role in the degenerative process of the tendon[92]. Savitskaya et al.,

also described the muscle response to tendon injury[92]. An increase in angiogenesis was measured and associated with an attempt to heal the trauma that has occurred in the attached tendon[6,93]. The timing of angiogenesis occurring in the SSP tendon after a complete tear remains to be characterized in the rabbit model and the contribution to muscle changes including fat accumulation have not yet been documented. The timeline studied the current experiments are measured in weeks whereas the trajectory of rotator cuff tear is not well documented. Events occurring early following a tear are not well described because patients do not seek medical attention until they become symptomatic[37–39].

In the rabbit model of rotator cuff tear, the SSP tendon response to injury is likely to involve the thoracoacromial artery and the suprascapular artery; the main blood vessels contributing to the blood supply of the distal SSP tendon[78,79]. Cook et al. showed that in the patellar tendon, neovascularization increased pain during loading of the joint[94]. In the context of human rotator cuff tears, Lakemeier et al., showed that increased vascular density can accelerate tendon degeneration by weakening the functional structure of the tendon[93]. Using biopsies harvested from patients undergoing surgical repair of a full-thickness SSP tendon tear, Lakemeier et al., quantified the change in vascular density in the SSP tendon using histology and described the relationship between vascularization and other markers for tendon degeneration such as fat accumulation and muscle atrophy[93]. Increased vascularization of tendons has been shown to contribute to pain and loss of function while being required for cell proliferation associated with healing. Results from those studies support a role for the vascular system in the early and late phases of the repair process of the rotator cuff tear as well as in the degeneration observed over time after tear. Our findings add to previous observations on the pathophysiology of rotator cuff tears. Both intramuscular fat accumulation and vascular changes co-localized in the distal portion

of the SSP muscle near the site of tendon detachment whereas changes were not notable in the middle and proximal regions of the SSP muscle.

Unexpectedly, surgical reattachment performed immediately after tendon detachment or at 4, 8, or 12 weeks after detachment did not change the number of vascular structures in the SSP muscle. The lack of vascular change in reattached specimens could be attributed to the restoration of tendon continuity and tensile strength of the SSP muscle and tendon. Our results suggest that the lack of mechanical stimulation in the detachment only group signal angiogenesis in the SSP muscle. As observed in muscle and bone, tendon is a mechanoresponsive tissue responding to the transfer of forces which are important to maintain the functional arrangement of its component cells[18]. When tendons are detached for an extended period of time, they degenerate because they are no longer mechanically stimulated by muscles[5]. Degeneration is expected to occur in the detachment only group since in detached muscles, no forces are transmitted to the tendon from the muscle. In the immediate reattachment group, tendon / bone interface is disrupted while maintaining tension in muscle and tendon by re-attachment. The immediate reattachment of the SSP tendon allows for forces to travel through the SSP musculotendinous unit. The maintenance forces and muscle stretching may prevent the triggering of angiogenesis in the tendon and muscle. In the delayed reattachment group, tendon to bone continuity is disrupted and the muscle retracts prior to surgical reattachment. Changes in vascularization could have occurred before the end of the healing period of 12 weeks following surgical reattachment but the current study was not designed to measure the timing of vascular changes and muscle atrophy.

Our results indicate that the persistence of intramuscular fat observed in reattachment groups is likely to involve mechanisms other than an increase in vascular density. Precursor cells for

skeletal muscle adipocytes have previously been identified and in some cases, their differentiation does not require vascularization[95]. For example, Gregory et al. have shown that adipocytes cultured in vitro, can develop in skeletal muscle cells originating from non-hematopoietic mesenchymal stem cells of the bone marrow and in the absence of vascularization[95]. Of specific interest in this study is the potential contribution of pericytes, FAPs, and SCs to the increase in intramuscular fat. The roles different progenitor cells play in intramuscular fat accumulation will be addressed later in the discussion. The cellular sources of skeletal muscle adipocytes accumulating in SSP muscle following SSP tendon detachment remains to be established.

During quantification of vascular density in the delayed reattachment group, I observed blood vessels with thick vascular walls in SSP muscle sections from the delayed reattachment group. The first method used to quantify the thickness of vessels walls was immunohistochemistry performed using CD31 stained specimens. The number of blood vessels with thick walls over the total number of blood vessels was reported as a percentage. An increased percentage of thick vascular structures was observed in the distal portion of the SSP muscle following 4 weeks of SSP tendon detachment plus 12 weeks after surgical reattachment. The increased vessel wall thickness was initially attributed to the smooth muscle layer and in subsequent experiments confirmed by staining with an antibody specific for actin of the α-smooth muscle cells where the average thickness of the medial layer of vascularization was measured. The observation of increased thickness partially confirmed our third hypothesis of an increase in vascular thickness localized to the distal portion of the SSP muscle closest to the tendon tear site. The increase in medial thickness was not limited to the distal portion of the SSP muscle at 4+12 and 12+12 weeks and was also significant in the proximal region of the SSP

muscle at 4+12 weeks of delayed reattachment. The middle region of the SSP muscle showed increased medial thickness in both the delayed reattachment and control specimens which aligns with the known anatomy of vascularization in the SSP muscle. The suprascapular artery enters in the middle region of the SSP muscle with the largest blood vessels and diverges to the distal and proximal region[74]. Thick vascular structures are normally found in the middle location and decrease in size as vascularization migrates toward the distal and proximal ends of the SSP muscle.

Vascular structures with increased thickness of the sub-endothelial layer were only observed in the delayed reattachment group. Vascular thickening has previously been described in association with hypertension and ageing but little is known about consequences on muscle physiology and pathology[61]. Vascular thickening is a natural occurrence during the ageing process where the medial thickness doubles in size between the 20 and 90 years of age in healthy individuals whereas patients suffering from hypertension will see a more pronounced increase in medial thickness over the same time period[61]. It has also been reported that increased vascular thickness can decrease vascular compliance, preventing proper secretory function of vascularization, potentially impacting fat accumulation[61,96]. Blood solutes are passed through the vascular endothelium through fenestrations between cells[61,96]. Medial thickening increases the permeability of the vascular endothelium and as a consequence alters the diffusion of soluble blood components during blood vessel contraction[61,96]. Pericytes, progenitors for adipocytes or skeletal myocytes, can accumulate in the sub-endothelial space and potentially contribute to intramuscular fat accumulation by migrating into the intramuscular space[64,66,97]. In addition, Birbrair et al., have shown that, following skeletal muscle injury in a mouse model pericytes resident in vascularization will differentiate into intramuscular adipocytes[64]. In the current

animal model of rotator cuff tear, focused on early time points and therefore acute inflammation, the surgical detachment could be responsible for the initial increase in vascularization while chronic inflammation, persisting after surgical reattachment, could be responsible for the increased vascular thickness[61,98]. Our observation of increased vascular wall thickness in association with healing of SSP tendon detachment after surgical reattachment warrants further investigation into the consequences of vascular thickening in the context of tendon and muscle changes associated with rotator cuff tear.

4.2 Supraspinatus Muscle Vascularization and Association with Intramuscular Fat

The second objective was to quantify the relationship between intramuscular fat accumulation and vascularization following SSP tendon detachment with or without surgical reattachment. Changes in SSP muscle vascularization were analyzed in the context of intramuscular fat accumulation using data previously published from the detachment only and delayed reattachment groups[26,51]. Data was not available for the detachment and immediate reattachment group. Results from the correlation analysis partially confirmed our hypotheses: following SSP tendon detachment increased vascularization of the SSP muscle was significantly correlated with intramuscular fat accumulation. No significant correlation was observed in the delayed reattachment group; intramuscular fat increased while the number of vascular structures returned to control values. The cascade of events, cellular and molecular participants all leading to intramuscular accumulation remain to be elucidated. In the current study, we measured increased vascular density and suggested a potential contribution to fat accumulation in the SSP muscle.

Published data on fat depots, other than the intramuscular depot, have described how adipocytes rely on free fatty acids and soluble blood components in vascularization to develop

and proliferate[66,99]. Potential mechanisms include the participation of FAPs[55]. FAPs are resident progenitor cells found in healthy adult skeletal muscle with the potential to differentiate into adipocytes or fibroblasts and are found neighbouring vascularization[55,56,67]. Following acute skeletal muscle injury in a mouse model, early FAP proliferation was observed and occurred prior to SCs proliferation[67]. As such, FAPs will fill the space between myofibers. If the myogenic differentiation is efficient and repairing the injured muscle, then FAPs will return to the dormant state[55,67]. If the myogenic differentiation is not efficient, then FAPs will differentiate into adipocytes and fibroblasts preventing muscle regeneration[55,67]. Liu et al., used a transgenic mouse model in which specimens underwent infraspinatus and SSP tendon transection to determine the origin of intramuscular fat[100]. These authors found that following a massive rotator cuff tear, 96% of cells expressing adipogenic markers in the SSP muscle were also expressing markers consistent with FAP progenitor cells[100]. Previous studies have provided evidence for FAP cells resident in skeletal muscles contributing to intramuscular fat accumulation following rotator cuff tears in a mouse model[55,67,101].

The mechanisms by which vascularization could contribute to intramuscular fat accumulation include pericytes, the contractile cells in vascular walls, which have been characterized as progenitors for adipocytes and myocytes in mouse models of muscle injury[64]. Some authors have found that pericytes accumulate in the endothelial space of developing vascular structures and differentiate into adipocytes and myocytes following muscle injury[64,66,97]. Two types of pericytes, both found in the tunica media layer of vascularization, have been characterized in the literature. In vitro experiments have shown that type 1 pericytes participated in fat accumulation while type 2 pericytes were associated with muscle regeneration[64]. Birbriar et al., have shown that by isolating type 1 and type 2 pericytes and culturing the isolated lineages in adipogenic

induction medium only type 1 pericytes are capable of differentiating into adipocytes[64]. It has been shown that in response to muscle injury type 1 and type 2 pericytes will become committed to their differentiation pathways; adipogenic or myogenic[73]. Aside from the role pericytes play in fat accumulation, they have also been shown to be associated with endothelial proliferation[64,65,97]. Another mechanism by which newly formed muscle vascularization could contribute to fat accumulation was proposed by Medici et al[102]. These authors identified vascular endothelial cells that can be converted into multipotent stem-like cells, progenitors for adipocytes[102]. These mechanisms were first noted in a mouse model when cartilage and bone exhibited endothelial markers[102]. Medici et al., isolated mouse endothelial cells and found that in the presence of growth factors expressed in all white blood cells, such as transforming growth factor, the endothelial cells could transform into stem-like cells with the ability to differentiate into adipocytes[102]. The relationship between vascularization and intramuscular fat we report is consistent with these outlined mechanisms. The sources of adipocytes contributing to increased intramuscular fat after tendon tear remains to be determined, including the potential contribution of mesenchymal stem cells residing in muscles with the capacity to differentiate into adipocytes upon muscle damage[102–104].

Results from our study and correlation analysis indicated that blood vessel increase contributed to intramuscular fat accumulation. Mechanisms other than increase in blood vessel density must contribute to the development and proliferation of intramuscular fat following rotator cuff tears. One potential contributor to fat proliferation is SCs[56,87,91]. SCs are resident in healthy skeletal muscle and upon damage, they can activate and proliferate into myocytes[56,87,91,104]. Although the primary function of SCs is to differentiate into myocytes in skeletal muscle, SCs can differentiate into adipocytes under certain conditions including the

presence of insulin[56]. The ability of SCs to differentiate into adipocytes may contribute to intramuscular fat accumulation following rotator cuff tears[56,87,91,104].

4.3 Limitations

This study has limitations associated with the chosen animal model, methodology used, and application to the clinical presentation of rotator cuff tears. First, the animal model imperfectly represents clinical rotator cuff disease: rabbits are quadrupeds and tendons were not degenerated after detachment and when analyzed[35]. Second, we only studied a complete detachment of the SSP tendon and the conclusions may not apply to partial tears. Thirdly, the observations are limited to at most 12 weeks following tendon detachment and 12 weeks after surgical reattachment; longer follow up times remain to be characterized[35]. Finally, the surgical cut of the SSP tendon is different than a tissue tear potentially evoking different mechanisms of repair. The overall sample size was large but multiple conditions of intervention, duration and control groups have reduced the statistical power to assess vascularization in groups.

Tendon degeneration, not present in the rabbit model studied here, likely represents the most important limitation to extrapolate findings in the clinical context of rotator cuff tear. Patients who experience rotator cuff tears are in most cases unaware of the duration or the severity of the tear[31]. Once a tear is suspected, patients may wait months for surgical reattachment. Using the delayed reattachment group, we attempted to mimic the delay between tear and repair but in Canadian clinical practices, the delay is measured in months or years and not weeks. Overall, animal models provide access to samples, can be used for testing new surgical techniques, and to describe disease processes but imperfectly represent the clinical presentation of rotator cuff tears.

When evaluating the methodology used in the study, limitations were noted. First, the muscle specimens used have been frozen for extended periods of time. The structure of myocytes might have been altered and assessing muscle volume was not possible. Inherent to the protocol for histology processing, the alcohol treatment of tissue sections led to the removal of fat and prevented us from performing the immunohistological analysis of intramuscular fat. Lastly, when analyzing the immunohistochemical staining of CD31 and αSMA on whole SSP muscle cross-sections, only a portion of the muscle sections was analyzed and corresponding to FOV positioned randomly on tissue sections.

4.4 Conclusions

In summary, this study investigated the change in vascular density in SSP muscle sections by histology and following SSP tendon detachment with or without reattachment and the association with intramuscular fat accumulation. There was a significant increase in vascularization following SSP tendon detachment that was not observed in both the immediate and delayed reattachment groups. In the detachment only group, the increase in vascularization was associated with intramuscular fat accumulation. In future, studies could be designed to manipulate the vascularization of the SSP muscle during rotator cuff tear and to measure the consequences on intramuscular fat accumulation to establish a cause and effect relationship. Our results support investigating the potential role of vascularization after tendon tear on intramuscular fat accumulation to mitigate the accumulation of intramuscular fat. By elucidating the mechanisms contributing to intramuscular fat accumulation, therapies can be designed to prevent or reverse intramuscular fat accumulation and improve long-term functional outcomes from rotator cuff repairs.

REFERENCES

1. Di Giacomo, G., Pouliart, N., Costantini, A. & De Vita, A. *Atlas of Functional Shoulder Anatomy*. **1,** (Springer, 2008).
2. Claudepierre, P. & Voisin, M. C. The entheses: Histology, pathology, and pathophysiology. *Jt. Bone Spine* **72,** 32–37 (2005).
3. DePalma, A. F. The classic. Surgical anatomy of the rotator cuff and the natural history of degenerative periarthritis. Surg Clin North Am. 1963;43:1507-1520. *Clin. Orthop. Relat. Res.* **466,** 543–551 (2008).
4. Levangie, P.K., and Norkin, C. . The Shoulder Complex. in *Joint Structure and Function: A Comprehensive Analysis* 245 (FA Davis, 2011).
5. Benjamin, M., Kaiser, E. & Milz, S. Structure-function relationships in tendons: A review. *J. Anat.* **212,** 211–228 (2008).
6. Nourissat, G., Berenbaum, F. & Duprez, D. Tendon injury: From biology to tendon repair. *Nat. Rev. Rheumatol.* **11,** 223–233 (2015).
7. Thomopoulos, S., Parks, W., Rifkin, D. & Derwin, K. Mechanisms of tendon injury and repair. *J. Orthop. Res.* **33,** 832–839 (2015).
8. Oatis, C. A. Kinesiology: The Mechanics & Pathomechanics of Human Movement. in 796 (Lippincott Williams & Wilkins., 2005).
9. Sharkey, N. A., Marder, R. A. & Hanson, P. B. The entire rotator cuff contributes to elevation of the arm. *J. Orthop. Res.* **12,** 699–708 (1994).
10. Kastelic, J., Galeski, A. & Baer, E. The multicomposite ultrastructure of tendon. *Connect. Tissue Res.* **6,** 11–23 (1978).
11. Buchanan, C. I. & Marsh, R. L. Effects of exercise on the biomechanical, biochemical and

structural properties of tendons. *Comp. Biochem. Physiol. - A Mol. Integr. Physiol.* **133,** 1101–1107 (2002).

12. Thorpe, C. T. *et al.* Helical sub-structures in energy-storing tendons provide a possible mechanism for efficient energy storage and return. *Acta Biomater.* **9,** 7948–7956 (2013).
13. Lichtwark, G. A. & Wilson, A. M. In vivo mechanical properties of the human Achilles tendon during one-legged hopping. *J. Exp. Biol.* **208,** 4715–4725 (2005).
14. Kvist, M. Achilles tendon injuries in athletes. *Sport. Med.* **18,** 173–201 (1994).
15. Kjær, M. *et al.* From mechanical loading to collagen synthesis, structural changes and function in human tendon. *Scand. J. Med. Sci. Sport.* **19,** 500–510 (2009).
16. Benjamin, M. & Ralphs, J. R. Fibrocartilage in tendons and ligaments—an adaptation to compressive load. *J. Anat* **193,** 481–494 (1998).
17. Yoon, J. H. & Halper, J. Tendon proteoglycans: Biochemistry and function. *J. Musculoskelet. Neuronal Interact.* **5,** 22–34 (2005).
18. Shaw, H. M. & Benjamin, M. Structure-function relationships of entheses in relation to mechanical load and exercise: Review. *Scand. J. Med. Sci. Sport.* **17,** 303–315 (2007).
19. Apostolakos, J. *et al.* The enthesis: a review of the tendon-to-bone insertion. *Muscles. Ligaments Tendons J.* **4,** 333–342 (2014).
20. Sano, H. *et al.* Structural disorders at the insertion of the supraspinatus tendon. Relation to tensile strength. *J. Bone Joint Surg. Br.* **80,** 720–725 (1998).
21. Koike, Y., Trudel, G. & Uhthoff, H. Formation of a new enthesis after attachment of the supraspinatus tendon: A quantitative histologic study in rabbits. *J. Orthop. Res.* **23,** 1433–1440 (2005).
22. Louati, H. *et al.* Supraspinatus tendon repair using anchors : a biomechanical evaluation in

the rabbit. *J. Orthop. Surg. Res.* **13,** 1–8 (2018).

23. Blevins, F. T., Djurasovic, M., Flatow, E. L. & Vogel, K. G. Biology of the rotator cuff tendon. *Orthop. Clin. North Am.* **28,** 1–16 (1997).

24. Lippe, J. *et al.* Inter-rater agreement of the Goutallier, Patte, and Warner classification scores using preoperative magnetic resonance imaging in patients with rotator cuff tears. *Arthrosc. - J. Arthrosc. Relat. Surg.* **28,** 154–159 (2012).

25. Goutallier, D., Postel, J.-M., Bernageau, J., Lavau, L. & Voisin, M.-C. Fatty muscle degeneration in cuff ruptures. Pre- and postoperative evaluation by CT scan. *Clin. Orthop. Relat. Res.* 78–83 (1994). doi:10.1097/00003086-199407000-00014

26. Trudel, G., Ryan, S., Rakhra, K. & Uhthoff, H. Extra- and intramuscular fat accumulation early after rabbit supraspinatus tendon division : Depiction with CT. *Radiology* **255,** 434–441 (2010).

27. Gilbert, F. *et al.* Comparing the MRI-based Goutallier Classification to an experimental quantitative MR spectroscopic fat measurement of the supraspinatus muscle. *BMC Musculoskelet. Disord.* **17,** 1–7 (2016).

28. Oh, L. S., Wolf, B. R., Hall, M. P., Levy, B. A. & Marx, R. G. Indications for rotator cuff repair: A systematic review. *Clin. Orthop. Relat. Res.* 52–63 (2007). doi:10.1097/BLO.0b013e31802fc175

29. Modules, S. T. Structure of Skeletal Muscle. *US Department of Health & Human Services* (2016). Available at: http://training.seer.cancer.gov/anatomy/muscular/structure.html. (Accessed: 3rd August 2016)

30. American Academy of Orthopaedic. Rotator Cuff Tears. *OrthoInfo* (2017). Available at: https://orthoinfo.aaos.org/en/diseases--conditions/rotator-cuff-tears-frequently-asked-

questions/.

31. Yamamoto, A. *et al.* Prevalence and risk factors of a rotator cuff tear in the general population. *J. Shoulder Elb. Surg.* **19,** 116–120 (2010).

32. Davis, M. E. *et al.* Simvastatin reduces fibrosis and protects against muscle weakness after massive rotator cuff tear. *J. Shoulder Elb. Surg.* **24,** 280–287 (2015).

33. Rush, L. N., Savoie, F. H. & Itoi, E. Double-row rotator cuff repair yields improved tendon structural integrity, but no difference in clinical outcomes compared with single-row and triple-row repair: a systematic review. *J. ISAKOSJoint Disord. Orthop. Sport. Med.* **2,** 260–268 (2017).

34. Deprés-tremblay, G. *et al.* Rotator cuff repair: a review of surgical techniques, animal models, and new technologies under development. *J. Shoulder Elb. Surg.* **25,** 2078–2085 (2016).

35. Derwin, K., Baker, A., Iannotti, J. & McCarron, J. Preclinical models for translating regenerative medicine therapies for rotator cuff repair. *Tissue Eng.* **16,** 21–31 (2010).

36. Woollard, J. D. *et al.* The ability of preoperative factors to predict patient-reported disability following surgery for rotator cuff pathology. *Disabil. Rehabil.* **39,** 2087–2096 (2017).

37. Safran *et al.* Changes in rotator cuff muscle volume, fat content, and passive. *Joseph P J. Bone Jt. Surg.* **87,** 2662–2670 (2005).

38. Sano, H., Ishii, H., Trudel, G. & Uhthoff, H. K. Histologic evidence of degeneration at the insertion of 3 rotator cuff tendons: A comparative study with human cadaveric shoulders. *J. Shoulder Elb. Surg.* **8,** 574–579 (1999).

39. Tempelhof, S., Rupp, S. & Seil, R. Age-related prevalence of rotator cuff tears in

asymptomatic shoulders. *J. Shoulder Elb. Surg.* **8,** 296–299 (1999).

40. Strobel, K. *et al.* Fatty atrophy of supraspinatus and infraspinatus muscles: accuracy of US. *Radiology* **237,** 584–589 (2005).

41. Fuchs, B., Weishaupt, D., Zanetti, M., Hodler, J. & Gerber, C. Fatty degeneration of the muscles of the rotator cuff: Assessment by computed tomography versus magnetic resonance imaging. *J. Shoulder Elb. Surg.* **8,** 599–605 (1999).

42. Mellado, J. M. *et al.* Surgically repaired massive rotator cuff tears: MRI of tendon integrity, muscle fatty degeneration, and muscle atrophy correlated with intraoperative and clinical findings. *Am. J. Roentgenol.* **184,** 1456–1463 (2005).

43. Gerber, C., Meyer, D. C., Schneeberger, a G., Hoppeler, H. & von Rechenberg, B. Effect of tendon release and delayed repair on the structure of the muscles of the rotator cuff: an experimental study in sheep. *J. Bone Joint Surg. Am.* **86–A,** 1973–1982 (2004).

44. Gladstone, J. N., Bishop, J. Y., Lo, I. K. Y. & Flatow, E. L. Fatty infiltration and atrophy of the rotator cuff do not improve after rotator cuff repair and correlate with poor functional outcome. *Am. J. Sports Med.* **35,** 719–728 (2007).

45. Lundgreen, K., Lian, O. B., Engebretsen, L. & Scott, A. Lower muscle regenerative potential in full-thickness supraspinatus tears compared to partial-thickness tears. *Acta Orthop.* **84,** 565–570 (2013).

46. Melis, B., Defranco, M. J., Chuinard, C. & Walch, G. Natural history of fatty infiltration and atrophy of the supraspinatus muscle in rotator cuff tears. *Clin. Orthop. Relat. Res.* **468,** 1498–1505 (2010).

47. Gumucio, J. P. *et al.* Aging-associated exacerbation in fatty degeneration and infiltration after rotator cuff tear. *J. Shoulder Elb. Surg.* **23,** 99–108 (2014).

48. Diebold, G., Lam, P., Walton, J. & Murrell, G. A. C. Relationship between Age and Rotator Cuff Retear. *J. Bone Jt. Surg. - Am. Vol.* **99,** 1198–1205 (2017).

49. Giambini, H. *et al.* Intramuscular fat infiltration evaluated by magnetic resonance imaging predicts the extensibility of the supraspinatus muscle. *Muscle and Nerve* 1–7 (2017). doi:10.1002/mus.25673

50. Goutallier, D., Postel, J. M., Gleyze, P., Leguilloux, P. & Van Driessche, S. Influence of cuff muscle fatty degeneration on anatomic and functional outcomes after simple suture of full-thickness tears. *J. Shoulder Elb. Surg.* **12,** 550–554 (2003).

51. Trudel, G., Ryan, S. E., Rakhra, K. & Uhthoff, H. K. Muscle tissue atrophy, extramuscular and intramuscular fat accumulation, and fat gradient after delayed repair of the supraspinatus tendon: A comparative study in the rabbit. *J. Orthop. Res.* **30,** 781–786 (2012).

52. Uhthoff, H., Coletta, E. & Trudel, G. Effect of timing of surgical SSP tendon repair on muscle alterations. *J. Orthop. Res.* **32,** 1430–1435 (2014).

53. Mendias, C. L. *et al.* Reduced muscle fiber force production and disrupted myofibril architecture in patients with chronic rotator cuff tears. *J. Shoulder Elb. Surg.* **24,** 111–119 (2015).

54. Smith, C., Kruger, M. J., Smith, R. M. & Myburgh, K. H. The Inflammatory Response to Skeletal Muscle Injury. *Sport. Med.* **38,** 947–969 (2008).

55. Joe, A. W. B. *et al.* Muscle injury activates resident fibro/adipogenic progenitors that facilitate myogenesis. *Nat. Cell Biol.* **12,** 153–163 (2010).

56. Sciorati, C., Clementi, E., Manfredi, A. A. & Rovere-Querini, P. Fat deposition and accumulation in the damaged and inflamed skeletal muscle: Cellular and molecular

players. *Cell. Mol. Life Sci.* **72,** 2135–2156 (2015).

57. Churchill, R. S. & Ghorai, J. K. Total cost and operating room time comparison of rotator cuff repair techniques at low, intermediate, and high volume centers: Mini-open versus all-arthroscopic. *J. Shoulder Elb. Surg.* **19,** 716–721 (2010).

58. Colvin, A. C., Egorova, N., Harrison, A. K., Moskowitz, A. & Flatow, E. L. National trends in rotator cuff repair. *J. Bone Jt. Surg. Am. Vol.* **94,** 227–33 (2012).

59. Iyengar, J. J. *et al.* Current trends in rotator cuff repair: Surgical technique, setting, and cost. *Arthrosc. - J. Arthrosc. Relat. Surg.* **30,** 284–288 (2014).

60. Hamrick, M. W., McGee-Lawrence, M. E. & Frechette, D. M. Fatty Infiltration of Skeletal Muscle: Mechanisms and Comparisons with Bone Marrow Adiposity. *Front. Endocrinol. (Lausanne).* **7,** 1–7 (2016).

61. Harvey, A., Montezano, A. C., Lopes, R. A., Rios, F. & Touyz, R. M. Vascular fibrosis in aging and hypertension: molecular mechanisms and clinical implications. *Can. J. Cardiol.* **32,** 659–668 (2016).

62. Campos, C. F. *et al.* Review: Animal model and the current understanding of molecule dynamics of adipogenesis. *Animal* **10,** 927–932 (2016).

63. Addison, O., Marcus, R. L., Lastayo, P. C. & Ryan, A. S. Intermuscular fat: A review of the consequences and causes. *Int. J. Endocrinol.* **2014,** 34–36 (2014).

64. Birbrair, A. *et al.* Role of pericytes in skeletal muscle regeneration and fat accumulation. *Stem Cells Dev.* **22,** 2298–2314 (2013).

65. Armulik, A., Genové, G. & Betsholtz, C. Pericytes: Developmental, physiological, and pathological perspectives, problems, and promises. *Dev. Cell* **21,** 193–215 (2011).

66. Frontini, A., Corvera, S. & Cinti, S. Origin of adipocyte prevursors from adipose vascular

endothelium. in *Methods in Molecular Biology* **456,** 65–81 (2013).

67. Natarajan, A., Lamos, D. & Rossi, F. Fibro/adipogenic progenitors: A double-edged sword in skeletal muscle regeneration Fibro / adipogenic progenitors. *Cell Cycle* **9,** 2045–2046 (2010).

68. Novotny, S. A. *et al.* Low intensity, high frequency vibration training to improve musculoskeletal function in a mouse model of duchenne muscular dystrophy. *PLoS One* **9,** (2014).

69. Klomps, L. V., Zomorodi, N. & Kim, H. M. Role of transplanted bone marrow cells in development of rotator cuff muscle fatty degeneration in mice. *J. Shoulder Elb. Surg.* **26,** 2177–2186 (2017).

70. Sonnabend, D. H. & Young, A. A. Comparative anatomy of the rotator cuff. *J. Bone Jt. Surg.* **91B,** 1632–1637 (2009).

71. Mathewson, M. A., Kwan, A., Eng, C. M., Lieber, R. L. & Ward, S. R. Comparison of rotator cuff muscle architecture between humans and other selected vertebrate species. *Clin. Cancer Res.* **217,** 261–273 (2014).

72. Uhthoff, H., Coletta, E. & Trudel, G. Intramuscular fat accumulation and muscle atrophy in the absence of muscle retraction. *Bone Joint Res.* **3,** 117–122 (2014).

73. Otrock, Z. K., Mahfouz, R. A. R., Makarem, J. A. & Shamseddine, A. I. Understanding the biology of angiogenesis: Review of the most important molecular mechanisms. *Blood Cells, Mol. Dis.* **39,** 212–220 (2007).

74. Korthuis, R. J. Anatomy of Skeletal Muscle and Its Vascular Supply. in *Skeletal Muscle Circulation* 13–18 (2011).

75. Conover, M. S., Hibbing, M. E. & Hultgren, S. J. *Metabolism of Human Diseases. Organ*

physiology and pathophysiology. (Springer, 2014). doi:10.1007/978-3-7091-0715-7

76. Pavelka, M. & Roth, J. *Functional ultrastructure an atlas of tissue biology and pathology*. (Springer, 2005).

77. Naidoo, N., Lazarus, L., De Gama, B. Z., Ajayi, N. O. & Satyapal, K. S. Arterial Supply to the Rotator Cuff Muscles. *Int. J. Morphol.* **32,** 136–140 (2014).

78. Lohr, J. F. & Uhthoff, H. K. The microvascular pattern of the supraspinatus tendon. *Clin. Orthop. Relat. Res.* **254,** 35–38 (1990).

79. Determe, D. *et al.* Anatomic study of the tendinous rotator cuff of the shoulder. *Surg. Radiol. Anat.* **98,** 195–200 (1996).

80. Longo, U. G. *et al.* Histopathology of the supraspinatus tendon in rotator cuff tears. *Am. J. Sports Med.* **36,** 533–538 (2008).

81. Hausman, G. J., Basu, U., Du, M., Fernyhough-Culver, M. & Dodson, M. V. Intermuscular and intramuscular adipose tissues: Bad vs. good adipose tissues. *Adipocyte* **3,** 242–255 (2014).

82. Rosen, E. D. & Spiegelman, B. M. What we talk about when we talk about fat. *Cell* **156,** 20–44 (2014).

83. Boundless Anatomy and Physiology. Blood Vessel Structure and Function. *lumencandela* (2018). Available at: https://courses.lumenlearning.com/boundless-ap/chapter/blood-vessel-structure-and-function/.

84. Boykin, R. E., Friedman, D. J., Higgins, L. D. & Warner, J. J. Suprascapular neuropathy. *J. Bone Jt. Surg.* **92,** 2348–2364 (2010).

85. Matsumoto, F., Uhthoff, H. K., Trudel, G. & Loehr, J. F. Delayed tendon reattachment does not reverse atrophy and fat accumulation of the supraspinatus-an experimental study

in rabbits. *J. Orthop. Res.* **20,** 357–63 (2002).

86. Uhthoff, H. K., Matsumoto, F., Trudel, G. & Himori, K. Early reattachment does not reverse atrophy and fat accumulation of the supraspinatus - An experimental study in rabbits. *J. Orthop. Res.* **21,** 386–392 (2003).

87. Sass, F. *et al.* Immunology guides skeletal muscle regeneration. *Int. J. Mol. Sci.* **19,** 835 (2018).

88. Tidball, J. G. Inflammatory processes in muscle injury and repair. *Am. J. Physiol. - Integr. Comp. Physiol.* **288,** 345–353 (2005).

89. Xia, C. *et al.* Analysis of blood flow and local expression of angiogenesis-associated growth factors in infected wounds treated with negative pressure wound therapy. *Mol. Med. Rep.* **9,** 1749–1754 (2014).

90. Li, Y., Cummins, J. & Huard, J. Muscle injury and repair. *Curr. Opin. Orthop.* **12,** 409–415 (2001).

91. Asakura, A., Rudnicki, M. A. & Komaki, M. Muscle satellite cells are multipotential stem cells that exhibit myogenic, osteogenic, and adipogenic differentiation. *Differentiation* **68,** 245–253 (2001).

92. Savitskaya, Y. *et al.* Effect of Angiogenesis-Related Cytokines on Rotator Cuff Disease : The Search for Sensitive Biomarkers of Early Tendon Degeneration. *Clin. Med. Insights Arthiritis Musculoskelet. Disord.* **4,** 43–53 (2011).

93. Lakemeier, S. *et al.* The association between retraction of the torn rotator cuff and increasing expression of hypoxia inducible factor 1α and vascular endothelial growth factor expression: an immunohistological study. *BMC Musculoskelet. Disord.* **11,** 230 (2010).

94. Cook, J. L. *et al.* Neovascularization and pain in abnormal patellar tendons of active jumping athletes. *Clin. J. Sport Med.* **14,** 296–299 (2004).

95. Gregory, C. A., Prockop, D. J. & Spees, J. L. Non-hematopoietic bone marrow stem cells: Molecular control of expansion and differentiation. *Exp. Cell Res.* **306,** 330–335 (2005).

96. Celermajer, D. S. *et al.* Aging is associated with endothelial dysfunction in healthy men years before the age-related decline in women. *J. Am. Coll. Cardiol.* **24,** 471–476 (1994).

97. Eilken, H. M. *et al.* Pericytes regulate VEGF-induced endothelial sprouting through VEGFR1. *Nat. Commun.* **8,** 1574 (2017).

98. Jerusalem, F., Rakusa, M., Engel, A. G. & MacDonald, R. D. Morphometric analysis of skeletal muscle capillary ultrastructure in inflammatory myopathies. *J. Neurol. Sci.* **23,** 391–402 (1974).

99. Christiaens, V. & Lijnen, H. R. Angiogenesis and development of adipose tissue. *Mol. Cell. Endocrinol.* **318,** 2–9 (2010).

100. Liu, X. *et al.* Investigating the cellular origin of rotator cuff muscle fatty infiltration and fibrosis after injury Corresponding author : *Muscles. Ligaments Tendons J.* **6,** 6–15 (2016).

101. Liu, X. *et al.* Investigating the cellular origin of rotator cuff muscle fatty infiltration and fibrosis after injury. *Muscles. Ligaments Tendons J.* **6,** 6–15 (2016).

102. Medici, D. *et al.* Conversion of vascular endothelial cells into multipotent stem-like cells. *Nat. Med.* **16,** 1400–1408 (2010).

103. Brioche, T., Pagano, A. F., Py, G. & Chopard, A. Muscle wasting and aging: Experimental models, fatty infiltrations, and prevention. *Mol. Aspects Med.* 1–32 (2015). doi:10.1016/j.mam.2016.04.006

104. Yin, H., Price, F. & Rudnicki, M. A. Satellite cells and the muscle stem cell niche. *Physiol. Rev.* **93,** 23–67 (2013).

CURRICULUM VITAE

Meaghan MacIntyre-Newell

Education

Master of Science – Biology — July 2018
University of Ottawa — Ottawa, ON

Bachelor of Science – Honours Cellular and Molecular Biology; Minor in Business Administration — April 2016
University of Ottawa — Ottawa, ON

Experience

Laboratory Technician – Level II — May 2018 – August 2018
University of Ottawa

Some cyanobacteria species have the ability to create toxins that pose a threat to the health of freshwater lakes. This is a significant problem in North America as the prevalence of algal blooms has increased in recent years threatening the health of wildlife and the general population

- Coordinated the proper shipment of samples, data, and protocols with collaborators in Minnesota, USA
- Optimized protocol for the processing and analysis of sediment samples to quantify presence of cyanobacterial species of interest using qPCR and ddPCR techniques
- Conducted field work to collect samples of lake sediment samples in the Ottawa region

Research Assistant – Department of Biology — May 2016 – May 2018
University of Ottawa — Ottawa, ON

Patient outcomes following surgical repair of a torn rotator cuff are typically low despite advances in current surgical techniques. The relationship between vascularization and intramuscular fat accumulation was defined to better understand the low surgical success rate and enable future improvements.

- Coordinated and executed a research project over a two-year period to achieve assigned objectives
- Optimized the use of a clinical diagnostic antibody to quantify vascularization of rotator cuff tears
- Developed analysis methods, using SPSS and R software, to quantify the change in vascularization and define the association between vascularization and intramuscular fat accumulation
- Advised undergraduate student researchers on best practices for completing research projects

Teaching Assistant – Department of Biology — May 2016 – Present
University of Ottawa — Ottawa, ON

Assisted in the instruction of four undergraduate courses in the Department of Biology.

- Corrected Molecular Biology examinations according to provided guidelines and supervised exam review sessions
- Lead weekly laboratory sessions for Introduction to Plant Diversity, Animal Form and Function, and Molecular Biology
- Coached students to better understand how key concepts and techniques apply to respective disciplines

Laboratory Assistant – The Bone and Joint Research Laboratory — May 2015 – April 2016
University of Ottawa — Ottawa, ON

Bedridden patients experience physical changes that are associated with the lack of use and loading of joints, muscles, and bones. Patient samples from The Ottawa Hospital Rehabilitation Center were used to characterize changes occurring as a result of deconditioning.

- Isolated leukocyte RNA from whole blood samples for transcriptome sequencing and downstream analysis to determine individual patient responses to deconditioning
- Created and maintained a detailed and organized database of all samples and results to be used for future analysis to quantify changes in transcriptome expression
- Dissected and processed frozen rabbit specimens to be used for histological evaluation of vascularization of rotator cuff tears

Awards

Hans K. Uhthoff, MD FRCSC Graduate Fellowship — January 2017
University of Ottawa Admission Scholarship — September 2011

Publications

MacIntyre-Newell, M., Uhthoff, H., Trudel, G., & Laneuville, O. Vascular structures and relationship to intramuscular fat in supraspinatus muscle following tendon detachment and reattachment: an experimental study in rabbits. Submitted.

Other Interests

City Stream Watch Volunteer — May 2016 – September 2016
Rideau Valley Conservation Authority — Ottawa, ON

Rideau Valley Conservation Authority works with volunteers to monitor and report information about the Ottawa Valley watershed since 2003.

- Conducted assessment of the stream habitat using physical and biological characteristics
- Identified aquatic benthic invertebrates and removed invasive species
- Assisted in stream rehabilitation and shoreline restoration